Transcriptional patterns of sexual dimorphism and in host developmental programs in the model parasitic nematode *Heligmosomoides bakeri*

Stephen M. J. Pollo[1,2], Aralia Leon-Coria[2,3], Hongrui Liu[2,3], Davide Cruces Gonzalez[2,3], Constance A. M. Finney[2,3], and James D. Wasmuth[1,2*]

[1]Faculty of Veterinary Medicine, University of Calgary, Calgary, Alberta, Canada

[2]Host-Parasite Interactions Research Training Network, University of Calgary, Calgary, Alberta, Canada

[3]Department of Biological Sciences, Faculty of Science, University of Calgary, Calgary, Alberta, Canada

* Corresponding author

E-mail: jwasmuth@ucalgary.ca (JDW)

Abstract

Heligmosomoides bakeri (often mistaken for *Heligmosomoides polygyrus*) is a promising model for parasitic nematodes with the key advantage of being amenable to study and manipulation within a controlled laboratory environment. While draft genome sequences are available for this worm, which allow for comparative genomic analyses between nematodes, there is a notable lack of information on its gene expression. Here, we have generated biologically replicated RNA-seq datasets from samples taken throughout the parasitic life of *H. bakeri*. We find extensive transcriptional sexual dimorphism throughout the fourth larval and adult stages of this parasite and identify alternative splicing, glycosylation, and ubiquitination as particularly important processes for establishing and/or maintaining sex-specific gene expression in this species. Further, we find sex-linked differences in transcription related to aging and oxidative and osmotic stress responses. Additionally, we observe a starvation-like signature among transcripts whose expression is consistently up-regulated in males, which may reflect a higher energy expenditure by male worms. We detect evidence of increased importance for anaerobic respiration among the adult worms, which coincides with the parasite's migration into the physiologically hypoxic environment of the intestinal lumen. Further, we hypothesize that oxygen concentration may be an important driver of the worms encysting in the intestinal mucosa as larvae, which not only fully exposes the worms to their host's immune system, but also shapes many of the interactions between the host and parasite. We find stage- and sex-specific variation in the expression of immunomodulatory genes and in anthelmintic targets. In addition to generating new hypotheses for follow-up experiments into the worm's behaviour, physiology, and metabolism, our datasets enable future more in-depth comparisons between nematodes to better define the utility of *H. bakeri* as a model for parasitic nematodes in general.

Author Summary

Parasitic nematodes (roundworms) that infect humans and livestock are a major health and economic burden but are challenging to study in a laboratory environment because of their required hosts. One strategy to get around this difficulty is to first study a rodent model to guide targeted experiments in the more difficult study system. *Heligmosomoides bakeri* is closely related to the nematode parasites of humans and livestock and naturally parasitizes mice. We have generated information on the expression of all the genes in this worm throughout the stages of its life when it is parasitic. This information allows us to examine how different the male and female worms are at the molecular level. We also describe major developmental events that occur in the worm, which extend our understanding of the interactions between this parasite and its host. We analyse the expression of genes known to be involved in interfering with host immune responses and others known to be targeted by drugs designed to kill worms. This new information will allow for better comparisons among nematodes to assess how well this rodent model system works for studying parasitic nematodes in general.

Introduction

Parasitic nematodes (roundworms) infect over 1 billion people, causing significant morbidity [1]. They also pose a significant threat to livestock, costing billions of dollars annually in production losses and treatment costs [2,3]. Yet, nematodes that parasitize humans or livestock are challenging to study in a controlled laboratory environment because the host is required to complete the parasite lifecycle. Studying the *in vivo* behaviour of the parasite during its infection requires samples to be taken from an infected host, not just obtaining eggs from feces. These samples can be technically challenging and expensive to obtain from large animals and not possible to obtain from humans. *Heligmosomoides bakeri* is well-suited to being a laboratory model because it is a natural parasite of mice, which are easily maintained in a laboratory environment, and there are protocols for maintaining *H. bakeri* in a laboratory environment. It is closely related to economically important parasites of livestock and the hookworm parasites of humans [4,5]. Furthermore, it can establish chronic infections in its mouse host, coarsely mimicking many other parasitic infections in a variety of hosts. Unravelling the responses to infection, adaptations to parasitism, and immunomodulatory strategies of *H. bakeri* will enable further development of this worm as a model for parasitic nematodes. Increased understanding of the biology of *H. bakeri* and what can be generalized to other related nematodes will then also enable preliminary experiments in *H. bakeri* to inform targeted experiments in harder to study parasites of large animals.

There has been an ongoing discussion as to the species designation for the lab isolates. Much of the literature on *H. bakeri* refers to the species as *H. polygyrus*, and a third name, *Nematospiroides dubius* has also been used. However, molecular studies demonstrate that the isolates widely used in laboratories are sufficiently genetically different to justify the original two species designation [6–8]. We confirm the species designation of the isolate used in this work (see Results). We, therefore, refer to the laboratory strain of this parasite as *H. bakeri*.

H. bakeri has a direct lifecycle with free-living and parasitic stages (Fig 1). Eggs present in feces hatch after 36-37 hours, releasing the L1 larvae which molt to L2 larvae 28-29 hours after hatching. After another 17-20 hours, the larvae partially molt resulting in ensheathed L3 worms that are the infective stage of the parasite. Once eaten by a rodent host, the L3 larvae exsheath and within 24 hours have penetrated the intestinal mucosa. The L3 larvae molt 90-96 hours (~4 days) after infection into L4 larvae which continue to develop in a granuloma formed by the host. A final molt 144-166 hours (~7 days) after infection results in adults which migrate out to the intestinal lumen [9]. The adult worms coil around the villi where they feed, mate, and lay the eggs which get passed with the feces [10]. The adults reside in the small intestine until they are expelled by the mouse, which can take anywhere from four to greater than 20 weeks depending on the strain of mouse [11].

Most studies on *H. bakeri* are motivated to understand its effects on its host's immune system; comparatively little is known about the worm itself. Two draft genome assemblies [12,13] are available for *H. bakeri*, which not only enable comparative genomic studies, but also allow for explorations of gene expression. A small set of 52 genes in *H. bakeri* (including chitinase, lysozyme, and glutathione S-transferases) was found to be differentially expressed between germ-free and pathogen-free mice using bulk RNA-seq of mixed-sex cultures, suggesting sensing of the microbial environment by the adult worms [14]. However, no transcriptomic information exists for other stages throughout the lifecycle or for sex-separated adults. Finally, attempts have been made to identify excreted/secreted products from

111 the worm that may have immunomodulatory potential, such as miRNAs within exosomes [15] and
112 proteins from separated and mixed-sex cultures [16].

113 Here, we have generated biologically replicated mRNA transcriptomes for both male and female
114 *H. bakeri* at four timepoints throughout their infection using RNA-sequencing (RNA-seq). The samples
115 span the fourth larval and adult stages of the worm (5, 7, 10, and 21 days post-infection). Our dataset
116 allows us to examine, for the first time, sexual dimorphism in the L4s and adults of this species at the
117 level of gene transcription. It also enables us to describe the major developmental changes and
118 processes that occur in the worms during their parasitic phase. Moreover, this dataset provides the first
119 publicly available resource to query the overall level of transcription of any gene of interest in this
120 species throughout the parasitic stages.

121

122 **Results and Discussion**

123 Confirming source species as *Heligmosomoides bakeri*

124 We mapped a randomly selected ten million RNA reads to the genome assemblies of *H. bakeri*
125 and *H. polygyrus*, each derived from single worms. We found that 93% of the reads mapped to *H. bakeri*
126 with 0.5% mismatch rate per base and 89% of the reads mapped to *H. polygyrus* with 2% mismatch rate
127 per base. When considering the alignment scores, 78% of reads mapped to better to *H. bakeri*, 8%
128 mapped better to *H. polygyrus*, and 14% mapped equally well to both. Collectively these demonstrate
129 that our nematode lab isolate is *H. bakeri*.

130

131 Mapping of bulk RNA-seq data and Differential Gene Expression (DGE)

132 Using the splice-aware aligner STAR, we mapped the RNA-seq reads to the *H. bakeri* genome
133 assembly obtained from WormBase ParaSite (PRJEB15396). Among all the datasets, 93.26 – 95.62% of
134 the reads uniquely mapped to the reference genome (Table 1), reflecting the high quality of the RNA
135 datasets (See S1 Text for additional quality control discussion). Moreover, the high mapping rate (which
136 does not include chimeric alignments) also indicates that the genome, while highly fragmented in 23647
137 scaffolds, contains the vast majority of the transcribed polyadenylated RNAs.

138 The sample groups were compared to each other using DESeq2 to find all transcripts that are
139 statistically significantly differentially expressed between conditions. The numbers of transcripts up- and
140 down-regulated between age-matched females and males or between adjacent timepoints among
141 females or males are shown in Fig 2. In general, differences between males and females increase with
142 age, whereas the biggest developmental differences are between the D7 and D10 timepoints for
143 females and the D5 and D7 timepoints for males.

144

145 Transcription level differences between male and female worms

146 In addition to the obvious significance to reproductive biology and nematode transmission,
147 sexual dimorphism has been found to be one of the biggest differences among lifecycle stages in a

148 variety of nematodes [17–20]. *H. bakeri* does not have a sex-specific chromosome, like a Y chromosome
149 as in many mammals or W chromosome in many birds. Rather, it has an XX/XO sex determination
150 system like *C. elegans* [21,22] and therefore, there are no male-specific or female-specific genes in *H.*
151 *bakeri*, only male-specific or female-specific expression of certain genes. To explore this sex-specific
152 gene expression, we looked for transcripts that were consistently up-regulated in the males or females.
153 These transcripts were statistically significantly differently transcribed ($p_{adj} < 0.05$ by DGE analysis, see
154 Methods and Fig 3) between males and females of the same age that had higher expression in all the
155 male samples (for up-regulated in males – URM) or in all the female samples (for up-regulated in
156 females – URF) and were found in relevant modules of the co-expression networks (S3 Fig). Throughout
157 all analyses, gene names used refer to *C. elegans* genes, with the corresponding *H. bakeri* locus tags
158 from WormBase ParaSite (HPOL_XXXXXXXXXX) in S27 Table. Among the 1084 URM transcripts (S3 Table)
159 were orthologs of genes in *C. elegans* with demonstrated association with males or demonstrated roles
160 in male development (S4 Table). Notable examples include the transcriptionally regulated male
161 development and patterning genes *mab-3* and *mab-23*; the male fate specification gene *her-1*; the male
162 mating behaviour associated genes *eat-4*, *cil-7*, and *mapk-15*; and the spermatogenesis-related genes
163 *spe-4*, *cpb-2*, *mib-1*, *fog-3*, and *cpb-1*. Additionally, among the URM transcripts were orthologs of genes
164 in *C. elegans* with roles in the regulation of gene expression, whose expression in this *H. bakeri* context
165 point to mechanisms by which male- or female-associated gene expression patterns may be established
166 and/or maintained. These include genes involved in alternative splicing like *prmt-9* and *rsp-8*;
167 glycosylation ZC250.2; and protein ubiquitination and protein folding *spop-1* and *cnx-1*. Finally, among
168 the URM transcripts are orthologs of genes in *C. elegans* with roles in starvation, including *ser-6*, *gcy-35*,
169 *pck-3*, *tre-2*, and *nemt-1*. Functional enrichment analysis of the entire URM set revealed 32 enriched
170 gene ontology (GO) terms that predominantly describe protein modification processes and
171 phosphorylation/dephosphorylation (S5 Table).

172 Among the 478 URF transcripts (S6 Table) were orthologs of genes in *C. elegans* with
173 demonstrated roles in hermaphrodite development or maternal processes (S7 Table). These include
174 genes involved in development of the vulva *soc-2* and *had-1*; development of the spermatheca *nhr-6*;
175 the sex determination pathway *fox-1*; oogenesis *csn-1*; ovulation *ipp-5*; egg formation *perm-4* and *gna-*
176 *2*; egg laying *bar-1*, *tmc-2*, and *sek-1*; and maternal roles in embryonic development *vha-7*. In contrast to
177 the males, URF transcripts contain different orthologs of *C. elegans* genes involved in alternative splicing
178 *ddx-15*; glycosylation *gale-1*, *ugt-64*, and ZK632.4; and protein ubiquitination *sli-1*, ZK430.7, and *cif-1*; as
179 well as orthologs of genes involved in translational regulation of gene expression *eif-2Bα*, K07A12.4, *eif-*
180 *3.E*, and *eif-3.D*. Moreover, rather than starvation-associated genes, URF transcripts include an ortholog
181 of a *C. elegans* gene involved in eating *eat-20*. Finally, among the URF transcripts are orthologs of genes
182 in *C. elegans* involved in stress responses including osmotic stress *nhr-1* and oxidative stress *aak-2*, *mek-*
183 *1*, *mlk-1*, *trx-2*. Functional enrichment analysis of the entire URF set revealed 18 enriched GO terms that
184 feature peroxisomes, mitochondria, and redox processes (S8 Table).

185 To further scrutinise the sex-specific gene expression, we defined male-specific transcripts as
186 transcripts that were statistically significantly differently transcribed and that had ≥ 10-fold higher
187 expression levels in all male samples compared to female samples of the same age (and vice versa for
188 female-specific transcripts). These criteria (significantly different expression between males and
189 hermaphrodites and ≥ 10-fold higher expression) when applied to *C. elegans* in a microarray study

190 identified 285 male-specific and 160 hermaphrodite-specific genes [23]. Here in *H. bakeri*, among the
191 160 male-specific transcripts (S2 Table) are 103 transcripts with no annotation information, highlighting
192 that many aspects of the male worms remain uncharacterized. Moreover, only two of these transcripts
193 have an ortholog in the *C. elegans* genome: HPOL_0000701801 which is in a many-to-one relationship
194 with W02D9.4 (an uncharacterized protein) and HPOL_0001987901 which is in a many-to-one
195 relationship with F29B9.7 (an uncharacterized protein). The remaining 57 transcripts come from 50
196 genes that are shown in S26 Table. Functions of these genes, inferred from their annotation, include
197 sperm production (HPOL_0001035601), male patterning (HPOL_0001902701), collagen synthesis and
198 cross-linking (HPOL_0000750501, HPOL_0001117101, HPOL_0001117201, HPOL_0001117301,
199 HPOL_0001117501), signalling cascades (HPOL_0000062301, HPOL_0000164101, HPOL_0000934501,
200 HPOL_0000982501, HPOL_0001599701, HPOL_0001692501, HPOL_0001834101, HPOL_0001912801),
201 and glycosylation (HPOL_0000317101). A high proportion of signalling cascade proteins has also been
202 noted for spermatogenesis-enriched transcripts in a *C. elegans* microarray study [24]. Notably only one
203 transcript fit the criteria as female-specific (HPOL_0000787001) and it is predicted to encode a
204 peptidase (S26 Table).

205 Finding orthologs of known male-related genes in URM and female-related (hermaphrodite in *C.*
206 *elegans*) genes in URF suggests that the filtering criteria used were appropriate to successfully recover
207 transcripts important for the males and females, respectively. The URM and URF sets are, therefore,
208 likely to reflect genuine differences between the males and females and not merely artifacts. The
209 different sets of transcripts used between the males and females for alternative splicing, glycosylation,
210 and protein ubiquitination point to the use of these processes to establish and/or maintain the
211 important differences in gene expression between the males and females as well as potentially generate
212 male/female isoforms of the targets of these gene products. It is surprising, however, to see oxidative
213 and osmotic stress signatures among the URF transcripts. The collection of the worms from their host
214 environment into medium is a stressful process that involves a transfer to a higher oxygen environment
215 (See S1 Text for additional discussion on intestinal oxygen) as a source of oxidative stress. Additionally, it
216 is possible the medium does not perfectly match the osmotic conditions of the mouse tissue and/or
217 lumen, thus providing a source of osmotic stress. However, it is unclear why the females would be more
218 responsive to these stresses than the males. Male worms have been found to die faster and in greater
219 proportion when exposed to oxidative stressors like arsenite for *C. elegans* [25] and peroxide for *H.*
220 *bakeri* [26]. Perhaps more sensitive and stronger stress responses in the female worms contributes to
221 their increased tolerance of the stressors.

222 It is also curious that we find a starvation-like expression signature among the URM transcripts.
223 It has been reported in *C. elegans* that the pharyngeal pumping rate decreases in males during mating
224 from 180 pumps per minute to 50 [27]. However, since the D5 and D7 males are larvae that are still
225 individually encysted in the intestinal tissue with no contact with a female they are not mating. Yet the
226 starvation-like expression signature is present at these stages as well, which contradicts a mating-
227 induced reduction in food intake in the males as an explanation for this transcript signature.
228 Additionally, starvation has been reported to inhibit mating behaviours in *C. elegans* males [28]. The
229 infection conditions we used here to obtain the worms are also used to generate eggs to grow to
230 infective L3 larvae to maintain the stock of worms in the laboratory, indicating that the adult worms do
231 mate under these conditions. It is therefore unlikely that the male worms are truly starved of food, and

using a bead-feeding assay, we found that males did feed (Fig 4 and S4 File). However, high feeding D10 adults were exclusively female (Fisher's exact test, p=0.04), while the males only fed at low rates. This suggests it is likely that males ingest less food than the females (even after accounting for differences in body size) resulting in a net energy deficit during the parasitic phase of their life. Alternatively, the males may have a higher energy expenditure in general compared to the females, resulting in more pronounced liberation of energy stores and a higher drive to seek food, both of which are associated with starvation responses. In support of this, male *C. elegans* were found to have higher carbohydrate metabolism through the glycolytic pathway than hermaphrodites [23].

The sheer number of transcripts that are significantly differentially expressed between males and females, both in URM + URF but also D10 (68.92%) and D21 (67.90%) (Fig 2 and Fig 5), reflects a significant level of sexual dimorphism at the transcriptional level in this nematode. We additionally analysed the RNA-seq datasets from *Haemonchus contortus* where the adult males and adult females were sequenced separately [20] and found 12669 of 21477 transcripts (58.99%) to be significantly differentially expressed between the adult males and females (using our same criteria as for *H. bakeri*). In *C. elegans*, a microarray study of adult males and hermaphrodites found 14488 / 26843 (53.97%) transcripts to be differentially expressed [23]. In all three nematodes, these proportions of transcripts that are differentially expressed between the adult sexes point to significant transcriptional sexual dimorphism in general. Our dataset additionally allows examination at the fourth larval stage, where sexual dimorphism is less prominent than in adults but is still notable (D5 – 33.58% and D7 – 55.74% transcripts differentially expressed between males and females; Fig 2). A microarray study from *C. elegans* L2, L3, and L4 worms that compared hermaphrodites to masculinized hermaphrodites (*tra-2(ar221ts)*; *xol-1(y9)* worms are strongly masculinized, fertile XX pseudomales) also found sexual dimorphism among the larval stages [29]. Though they identified fewer genes as sex-regulated than we have (possibly because they focused on somatic tissues while excluding germline tissues, and/or because of the lower sensitivity of microarrays compared to RNA-seq, and/or because of differences between the two species), they also found fewer genes to be sex-regulated among the larvae compared to adults, as well as many more male-enriched genes than hermaphrodite-enriched genes: both trends that we see here in *H. bakeri*. The greater number of male-enriched genes was postulated to be a consequence of the suppressive nature of the TRA-1 master sex-regulator in *C. elegans*, a gene that *H. bakeri* has a one-to-one ortholog of (HPOL_0000251701). These commonalities between the two worms support the view that TRA-1 suppressing male developmental programs in XX worms is a common feature among nematodes, whether they are dioecious like *H. bakeri* or androdioecious like *C. elegans*. Moreover, the same study found little overlap between the differentially expressed genes detected at early vs late larval stages [29]. This suggests significant, unexplored, sexual dimorphism exists even in the morphologically indistinct larval stages of other nematodes. Given the transcriptional sexual dimorphism in these nematodes, male/female differences should be taken into consideration in all future experiments, especially in dioecious species like *H. bakeri* or *H. contortus* where males and females exist in roughly uniform proportion.

Developmental transcriptional changes

272 The timepoints throughout infection for the samples used here include when *H. bakeri* larvae
273 are encysted in the intestinal tissue (D5 and D7) and when the adults have emerged into the lumen (D10
274 and D21). To identify the transcriptional changes that occur throughout this final phase of development
275 we defined, for both the males and the females, a set of transcripts up-regulated in the adults (lumen-
276 dwelling) and a set of transcripts up-regulated in the larvae (tissue-dwelling). To be considered up-
277 regulated in tissue-dwelling males (URTDM), transcripts had to: i) have higher expression in all D5 and
278 D7 male samples than in all D10 and D21 male samples, ii) be in relevant modules of the co-expression
279 networks (S3 Fig), and iii) have statistically significantly different expression in either of the tissue-
280 dwelling vs lumen-dwelling pairwise comparisons being considered (See Methods and Fig 6). To be
281 considered up-regulated in the lumen-dwelling males (URLDM), transcripts had to: i) have higher
282 expression in all D10 and D21 male samples than in all D5 and D7 male samples, ii) be in relevant
283 modules of the co-expression networks (S3 Fig), and iii) have statistically significantly different
284 expression in either of the tissue-dwelling vs lumen-dwelling pairwise comparisons being considered.
285 The same filtering criteria were applied to the female samples to find the transcripts up-regulated in the
286 tissue-dwelling females (URTDF) and up-regulated in the lumen-dwelling females (URLDF).

287 Among the 1829 URTDM transcripts (S9 Table) were orthologs of genes in *C. elegans* with
288 demonstrated roles in muscle development *lev-11*; epithelial development *ltd-1* and *efn-2*; cuticle
289 synthesis and molting *dpy-31*, *phy-2*, *tsp-15*, *fkb-3*, and numerous cuticlins and collagens; and male tail
290 development *lon-8* and *mab-7* (S10 Table). Additionally, among URTDM transcripts were orthologs of
291 genes in *C. elegans* with roles in environmental sensing *nep-2* and signal transduction *rrc-1* and *pde-6*.
292 Functional enrichment analysis of the entire URTDM set revealed 33 enriched GO terms that featured
293 the plasma membrane and cuticle synthesis, including structural constituents and procollagen-proline
294 dioxygenase activities (S11 Table). Within the 3264 URTDF transcripts (S12 Table) were orthologs of
295 genes in *C. elegans* with known roles in muscle development *unc-52* and *stn-1*; epithelial development
296 *efn-2*; nervous system development *irx-1*, *grdn-1*, *mig-13*, *kal-1*, *mnr-1*, and *mig-1*; cuticle synthesis and
297 molting *bus-19*, *phy-2*, *mlt-7*, *zmp-2*, and numerous cuticlins and collagens; and regulation of body size
298 and length *mua-3*, *sma-6*, and *lon-8* (S13 Table). Additionally, among URTDF transcripts were orthologs
299 of genes in *C. elegans* with roles in aerobic respiration and oxygen sensing *ucr-2.3*, *isp-1*, *pdl-1*;
300 environmental sensing *nep-2*; and nutrient absorption *sms-5*. Functional enrichment analysis of the
301 entire URTDF set revealed 67 enriched GO terms that featured oxygen binding and transport, cuticle
302 synthesis, and nervous system development (S14 Table). The URTDM and URTDF sets share 1560
303 transcripts (S15 Table). Functional enrichment of the shared up-regulated in tissue-dwelling worms
304 transcripts revealed 31 enriched GO terms that feature adhesion, cuticle and molting cycle, and oxygen
305 binding and transport (S16 Table).

306 Among the 2986 URLDM transcripts (S17 Table) was an ortholog of the *C. elegans*
307 spermatogenesis-related gene, *ubxn-2*. Additionally, among the URLDM transcripts were orthologs of
308 genes in *C. elegans* with roles in the cuticle *col-36*; and metabolism *sucg-1* and *tre-1* (S18 Table).
309 Functional enrichment analysis of the entire URLDM set revealed 64 enriched GO terms that feature
310 phosphorylation/dephosphorylation, ubiquitin ligase activity, and protein modification processes (S19
311 Table). Among the 5925 URLDF transcripts (S20 Table) were orthologs of genes in *C. elegans* with known
312 roles in adult gonad maintenance and development *ippk-1*, *mys-1*, *tin-9.2*, and *evl-20*; egg laying *fahd-1*
313 and *rfp-1*; maternal factors for embryonic development *mel-32*, *par-4*, *dnc-4*, and *emb-4*; and germline

314 maintenance and gametogenesis *clk-2*, *dvc-1*, *stau-1*, and *etr-1* (S21 Table). Additionally, among URLDF
315 transcripts were orthologs of genes in *C. elegans* with roles in mRNA splicing *prcc-1* and *prp-19*;
316 translation *eif-3.C*; protein deubiquitination *otub-1*; heparan sulfate metabolism *hst-2* and *pst-2*; and
317 negative regulation of aerobic respiration *blos-1* or response to reoxygenation *stl-1*. Functional
318 enrichment analysis of the entire URLDF set revealed 262 enriched GO terms that feature regulation of
319 gene expression (RNA processing, glycosylation, ubiquitination, histone modification, and translation
320 terms) and cell cycle terms (S22 Table). The URLDM and URLDF sets share 1007 transcripts (S23 Table).
321 Functional enrichment of the shared up-regulated in lumen-dwelling worms transcripts revealed 59
322 enriched GO terms that feature cell cycle and ubiquitin protein catabolic processes (S24 Table).

323 Since the tissue-dwelling worms are still developing, finding in URTDM and URTDF orthologs of
324 genes in *C. elegans* with known roles in development suggests that the filtering criteria used were
325 appropriate to successfully recover transcripts important for the tissue-dwelling worms. Likewise,
326 finding in URLDM and URLDF orthologs of genes in *C. elegans* with known roles in gametogenesis and
327 reproduction suggests that the filtering criteria used were appropriate to successfully recover transcripts
328 important for the lumen-dwelling worms. It is, therefore, worth additional investigation into the
329 importance heparan sulfate metabolism may be playing in the adult female worms and into whether the
330 additional phosphorylation and dephosphorylation activities in the adult males are purely a
331 consequence of spermatogenesis or whether this also reflects other critical male processes.

332 It has been reported previously that nematodes are capable of anaerobic respiration (ex. *Ascaris*
333 *suum* [30], *Haemonchus contortus* [31], *C. elegans* [32]). Additionally, a study comparing three free-
334 living nematodes (*C. elegans*, *Pristionchus pacificus*, and *Panagrolaimus superbus*) and one plant-
335 parasitic nematode (*Bursaphelenchus xylophilus*) found the parasitic nematode survived anaerobic
336 conditions much longer than the free-living ones [33], suggesting surviving low oxygen environments
337 may be a particularly important adaptation for parasitic nematodes compared to their free-living
338 relatives. The enriched GO terms involving oxygen binding, transport, and utilization among URTDM and
339 URTDF transcripts (and the lack of such terms among the URLDM and URLDF transcripts) suggests that
340 an increased role for anaerobic respiration, at least in *H. bakeri*, occurs during the transition from the L4
341 to the adult stage. This transition is when the worms migrate from the intestinal mucosa, a
342 physiologically aerobic environment, to the intestinal lumen, a physiologically hypoxic environment [34]
343 (See S1 Text for additional discussion on intestinal oxygen). The transition from the L4 to adult stage is
344 also when the final molt occurs, along with synthesis of the final cuticle. This aligns with the abundance
345 of collagens, cuticlins, and cuticle-related GO terms that are enriched in the URTDM and URTDF
346 transcripts. Among the many steps involved in cuticle synthesis is the modification of certain proline
347 residues in the collagen molecules to 4-hydroxyproline [35], a process requiring molecular oxygen
348 [35,36], and the process most likely reflected in the enriched GO terms involving procollagen-proline
349 dioxygenase activity (S11, S14, S16 Tables). Characterized human enzymes that perform this function
350 (prolyl 4-hydroxylases) catalyze the reaction L-proline + 2-oxoglutarate + O_2 → 4-hydroxyproline +
351 succinate + CO_2 [36]. In *H. bakeri*, this occurs when the L4 worms are in a physiologically aerobic
352 environment and all other molts and synthesized cuticles in *H. bakeri* occur outside the host in a fully
353 aerobic environment. We hypothesize that the levels of oxygen in the intestinal lumen are insufficient to
354 support this collagen modification (and/or *H. bakeri* is unable to scavenge the required oxygen), which
355 suggests that cuticle synthesis is a strictly aerobic process. In support of this, prolyl 4-hydroxylases are

356 also involved in oxygen sensing through their oxygen-dependent modification and destruction of the
357 hypoxia inducible factor [36], a transcription factor that is induced in the host epithelial cells lining the
358 intestinal tract [34]. If luminal oxygen is indeed insufficient to support prolyl 4-hydroxylase activity, the
359 need for molecular oxygen to get through the final molt within the host could be a driver of the worms
360 encysting in the intestinal mucosa, a phenomenon that fully exposes the worms to the host immune
361 system (in contrast to the lumen which is beyond the reach of many immune effectors). Many parasitic
362 nematodes encyst within host tissue (ex. *Cooperia punctata* [37] and *Trichinella spiralis* [38], which both
363 invade the intestinal mucosa during their development), migrate through aerobic host tissues (ex.
364 *Ascaris lumbricoides* [39], *Necator americanus* [40], and *Nippostrongylus brasiliensis* [41], which all
365 migrate through circulatory and pulmonary tissues), or actively seek host blood (ex. *Haemonchus*
366 *contortus* [42] and *Ancylostoma duodenale* [40]), which would all provide a rich source of molecular
367 oxygen for synthesis of the final cuticle regardless of where the adults ultimately reside in the host.

368 Since our timepoints span much of the adult life of *H. bakeri*, we investigated potential gene
369 expression signatures of aging. The expression in *H. bakeri* of orthologs of genes in *C. elegans* that have
370 been implicated in aging shows that our *H. bakeri* dataset has insufficient samples across the adult stage
371 to robustly identify genes implicated in aging based on their expression patterns alone (S4 Fig and S1
372 Text for additional discussion on aging-related gene expression). However, the *H. bakeri* orthologs of the
373 *C. elegans* IIS pathway [43] show marked differences in expression pattern between the males and the
374 females (Fig 7), suggesting that molecular pathways involved in aging may differ between males and
375 females. It has been reported previously in *C. elegans* that transcription of certain isoforms (d/f) of the
376 *daf-16/FOXO* transcription factor is affected in a sex-specific manner by TRA-1 to increase *daf-16* activity
377 [44]. Our results, however, show a notable decrease in the transcription of *daf-16* (HPOL_0000379201)
378 in *H. bakeri* females upon reaching adulthood, in contrast to steadily increasing transcription in the
379 males as their parasitic life progresses (Fig 7). It is worth noting, however, that in the current *H. bakeri*
380 genome annotation there is only one isoform predicted for *daf-16* (HPOL_0000379201), which
381 corresponds to the b/c isoforms in *C. elegans* (data not shown), highlighting that the annotations in *H.*
382 *bakeri* still need work.

383

384 Expression of immunomodulatory genes and anthelmintic target genes

385 The majority of the male/female and developmental transcriptional responses described here
386 center around the intestine, hypodermis, and gonad tissues of the worms. An estimate of tissue sizes in
387 *C. elegans* places these three tissues as the largest in the worm, cumulatively accounting for more than
388 three quarters of the worm's tissue volume [45]. Since bulk RNA-seq pools together RNA from the whole
389 worm, it is not surprising that the signatures of these tissues dominate our results. However, one
390 phenotype of particular interest in *H. bakeri*, immunomodulation of its host, is not necessarily governed
391 by these tissues. While some of the excreted/secreted products of *H. bakeri* with immunomodulatory
392 activity were found to originate in the intestine (vesicles containing microRNAs) [15], the
393 excreted/secreted proteins with described or implied immunomodulatory activity have no
394 demonstrated tissue of origin in the worm. Excreted/secreted proteins in other parasitic worms have
395 been found to originate from the uterine fluid and/or other sources, like the secretory apparatus [46].
396 Therefore, a possible source tissue for *H. bakeri* immunomodulatory proteins are excretory cells, which

397 make up a very small proportion of whole *C. elegans* [45]. Comparative analyses may be able to uncover
398 differential signal originating from rarer cell types like the excretory cells, especially if the differences
399 between conditions are extreme. We therefore investigated the expression of loci that have been
400 associated with immunomodulatory activity to see what comparisons or expression patterns might
401 identify other immunomodulatory candidates. Most of the excretory/secretory proteins in *H. bakeri* that
402 have been associated with immunomodulatory activity have not been identified but are members of
403 certain classes of genes with common annotation descriptions (S25 Table). We therefore included all loci
404 that matched each description. Expression patterns within these groups of genes vary considerably (S5
405 Fig). Moreover, even among described immunomodulatory proteins there are opposing expression
406 patterns that exclude any one pairwise comparison from being more likely to identify
407 immunomodulatory candidates (Table 2, Fig 8, and S1 Text for additional discussion on
408 immunomodulatory gene expression). Hb-TGM-6 was identified as HPOL_0001864701 [47], which has
409 higher expression in lumen-dwelling males than in tissue-dwelling males (as found with mixed-sex
410 protein secretion) as well as sex-linked differences in expression (Fig 8 and S5 Fig). HbARI was identified
411 as HPBE_0000813301 in the PRJEB1203 annotation [48], which when aligned against PRJEB15396
412 corresponds to HPOL_0001636401 (Fig 9), which has higher expression in the tissue-dwelling worms
413 than in the lumen-dwelling worms (Fig 8 and S5 Fig). These data demonstrate that the expression of
414 these two families of immunomodulators is tightly controlled. Moreover, our findings are consistent
415 with the parasite's need for these immunomodulators during infection. HbARI interferes with the
416 release of IL-33, an alarmin which initiates the immune response to nematode infection and whose
417 release is triggered by tissue damage [48]. IL-33 was found to be produced early in murine infection with
418 the nematode *Trichuris muris*, which promotes worm expulsion in resistant mice [49]. Production and
419 release of HbARI early in *H. bakeri* infection, when the worms are in the tissue and causing damage,
420 helps regulate the host response to the worm's damage and allows the worms to persist long enough to
421 make it into the lumen where they are not causing the same level of tissue damage. In contrast, Hb-TGM
422 is needed later in infection, where it stimulates TGF-β signalling and interferes with regulatory immune
423 cells [47].

424 It is likely that *H. bakeri* secretes other proteins with immunomodulatory activity. However,
425 these are unlikely to have uniform expression throughout the worm, may very well be secreted by a
426 handful of specialized cells, and are not specific to males, females, or a lifecycle stage sampled here.
427 Therefore, a higher resolution technique, like single-cell RNA-seq, would be needed to identify other
428 immunomodulatory candidates based on their transcriptional expression patterns.

429 We also analyzed the expression profiles of known anthelmintic drug targets (Table 3 and Table
430 4). Of note, the majority of the drug targets have medium or low levels of transcription in both sexes at
431 all stages sampled (TPMs range from 0 to 34856.8, with the top 10% of transcript expression
432 corresponding to a TPM ≥ 66.9, top 30% corresponding to a TPM ≥ 14.7, and top 50% corresponding to a
433 TPM ≥ 2.8). It is unclear if the medium and low expression reflect medium/low expression throughout
434 the whole worm or high expression in a few cells and very low expression in the major tissues of the
435 worms. The three highly expressed transcripts (top 10%) are the targets of benzimidazoles and a
436 neuropeptide GPCR. Expression of the majority of the drug targets varies significantly between at least
437 two of the sampled timepoints in both males and females, which may indicate higher drug efficacy on
438 worms of particular ages or stages of development.

439

440 **Conclusions**

441 By separating the males and females at each timepoint in our biologically replicated mRNA
442 transcriptomes that span the parasitic phase of the *H. bakeri* lifecycle, we have been able to examine
443 sexual dimorphism in this species and examine development without masking important sex-specific
444 signals. We have uncovered inconsistencies in the available genome annotations for *H. bakeri*, along
445 with other limitations that demonstrate a need to continue the work of annotating available genome
446 sequences for this organism. We have identified processes that are key in establishing and/or
447 maintaining sex-specific gene expression in this worm, without having sex-specific genes, including
448 alternative splicing, glycosylation, and ubiquitination. Additionally, we find stronger oxidative and
449 osmotic stress responses among female worms, potentially accounting for their previously reported
450 better survival of oxidative assault. We hypothesize that oxygen concentration may be an important
451 factor in the encysting behaviour of larval stage *H. bakeri* (in order to get through their last molt), a
452 factor that could be more general among parasitic nematodes. We demonstrate the advantage of
453 quantifying the levels of all transcripts in the worm by highlighting previously unknown transcription
454 differences in immunomodulatory genes between worm sexes and lifecycle stages. Finally, the level of
455 transcriptional sexual dimorphism we observe in this species (as well as in *H. contortus* and *C. elegans*)
456 highlights the need to consider male/female differences in the worms in future experiments with
457 dioecious nematodes.

458

459 **Materials and Methods**

460 Mice and parasites

461 Male C57Bl/6 mice aged 6-8 weeks (bred and maintained at the animal care facility, Department
462 of Biological Sciences, University of Calgary) were used. All animal experiments were approved by the
463 University of Calgary's Life and Environmental Sciences Animal Care Committee (protocol AC17-0083).
464 All protocols for animal use and euthanasia were in accordance with the Canadian Council for Animal
465 Care (Canada). Infected mice were orally gavaged with 300 third stage *Heligmosomoides bakeri* larvae
466 (maintained in house, original stock was a gift from Dr. Lisa Reynolds, University of Victoria, Canada) and
467 euthanized at either 5, 7, 10, or 21 days post initial infection. Worms were removed from the intestinal
468 tract, placed in Dulbecco's modified eagle's medium – high glucose (Sigma cat. D5796) where they were
469 sexed and counted. The number of worms in each sample is shown in Table 1. Worms were snap frozen
470 and kept at -80°C until RNA isolation.

471

472 RNA isolation and quality control

473 Worms were lysed by adding 100 µL of Trizol and homogenizing in dry ice three times, for a total
474 of three freeze-thaw cycles and a final volume of 300 µL. The mixture was centrifuged and the
475 supernatant was collected into a new tube where RNA was extracted using the Zymo Direct-zol RNA
476 Miniprep kit (Cat No. R2050) following the manufacturer's instructions. RNA was digested once with

477 DNase during the isolation, which has been found to sufficiently deplete DNA so as to not interfere with
478 downstream RNA-seq analyses [50]. The RNA was then cleaned using the Zymo RNA Clean and
479 Concentrator -5 kit (Cat No. R1015) following the manufacturer's instructions. Quantity and quality of
480 the total RNA was assessed on an Agilent 2200 TapeStation RNA ScreenTape following the
481 manufacturer's instructions.

482

483 Library preparation and sequencing

484 Libraries were made from suitable RNA samples using the NEBNext Ultra II Directional RNA
485 Library Prep Kit following the manufacturer's instructions. Libraries were multiplexed and paired-end
486 sequenced on an Illumina NovaSeq with a S2 flow cell or SP flow cell for 300 cycles (2x150bp) using the
487 v1.5 reagent kit, following the manufacturer's instructions. The resulting reads were deposited in the
488 SRA under the accession number PRJNA750155.

489

490 Species assignment

491 Ten million reads were randomly selected from all the libraries using seqtk [cite]. They were
492 mapped to genome assemblies for *H. bakeri* (GCA_947359475.1_nxHelBake1.1, Lewis Stevens personal
493 communication) and *H. polygyrus* (GCA_947396885.1_ngHelPoly1.1, Lewis Stevens personal
494 communication) using STAR v2.7.10b with default parameters [51]. The STAR alignment score is
495 recorded in the 'AS' for each read and a custom Perl script was used to determine to which assembly
496 each read mapped better to.

497

498 Aligning RNA-seq reads and counting reads per transcript

499 RNA-seq reads were aligned to the *H. bakeri* genome assembly obtained from WormBase
500 ParaSite (PRJEB15396) using the splice-aware aligner STAR v2.7.3a [51]. The resulting BAM alignment file
501 was used as input for the program featureCounts v2.0.3 [52] to count the fragments overlapping each
502 transcript. Second stranded counts were used only on read pairs with both ends aligned in the proper
503 orientation and fragments overlapping multiple transcripts were fractionally counted among all
504 matches. RNA-seq reads were aligned to the transcript sequences predicted by the annotation
505 accompanying the *H. bakeri* genome assembly PRJEB15396 using the non-splice-aware aligner bwa
506 v0.7.17-r1188. The commands used in all analyses can be found in S2 File.

507

508 Differential gene expression analysis

509 Read counts per transcript were rounded to the nearest integer and differential transcript
510 expression was analyzed using DESeq2 v1.30.1 [53]. Within each pairwise comparison, transcripts with a
511 false discovery rate adjusted p-value of less than 0.05 were considered differentially expressed.

512 For male / female comparisons (MS, FS, URM, and URF), pairwise comparisons considered
513 included D5M vs D5F, D7M vs D7F, D10M vs D10F, and D21M vs D21F. Transcripts that were
514 differentially expressed in all four pairwise comparisons were selected. Those that had ≥ 10 fold higher
515 expression in the male samples of the pairwise comparisons were retained as the MS transcripts. Those
516 that had ≥ 10 fold higher expression in the female samples of the pairwise comparisons were retained as
517 the FS transcripts. Those that had higher expression in the male samples of the pairwise comparisons
518 and were in unsigned network modules M3 or M5 and were in signed network modules M3 or M4 were
519 retained as the URM transcripts. Those that had higher expression in the female samples of the pairwise
520 comparisons and were in unsigned network modules M1 or M9 and were in signed network modules
521 M1, M6, or M9 were retained as the URF transcripts.

522 For developmental comparisons (URTDM, URTDF, URLDM, and URLDF) counts per transcript in
523 the DESeq2 object were VST-transformed to yield expression estimates for every transcript in every
524 sample. For males and females separately, the expression estimates were then compared between
525 every replicate of D5 and D7 samples vs every replicate of D10 and D21 samples to select all transcripts
526 that were up-regulated in the tissue-dwelling phase or the lumen-dwelling phase. Transcripts were then
527 filtered using the co-expression modules (URTDM – unsigned modules M2, M3, or M6 and signed
528 modules M2, M6, M7, or M8; URLDM – unsigned modules M3, M4, or M5 and signed modules M3, M4,
529 or M5; URTDF – unsigned modules M2, M3, M5, M6, M8, or M10 and signed modules M2, M3, M4, M7,
530 M8, or M10; URLDF – unsigned modules M1, M3, M4, M5, or M7 and signed modules M1, M3, M5, M6,
531 or M9). Transcripts that were differentially expressed in at least one of the D7 vs D10 or D5 vs D21
532 pairwise comparisons were retained.

533

534 Co-expression network analysis

535 Read counts per transcript were normalized into fragments per kilobase per million mapped
536 reads (FPKM) using the R package countToFPKM v1.0. The top 75% of transcripts by expression value
537 were then grouped into co-expression modules with the R package CEMiTool v1.14.1 [54] using the
538 FPKM values, using the variance-stabilizing transformation and the pearson correlation. Modules were
539 visualized in R to allow determination of the pattern of module enrichment across the sample groups.

540

541 Identification of orthologs in *C. elegans*, Gene ontology functional enrichment analysis, Anthelmintic
542 target identification, TPM calculation

543 All orthologs between *H. bakeri* and *C. elegans* were retrieved from WormBase Parasite. When
544 transcripts of interest were identified in *H. bakeri* for which there was a one-to-one ortholog in *C.*
545 *elegans*, the function of the *C. elegans* gene was identified through manual literature search.

546 GO terms enriched in any set of transcripts of interest were identified using the R package
547 gprofiler2 v0.2.1 [55].

548 Orthologs of known anthelmintic target genes, as previously identified in *C. elegans* [56], were
549 retrieved from WormBase Parasite. Additional targets of interest were taken from [57]. With the *H.*

bakeri locus tags, expression of each target was examined. TPM (transcripts per million) were calculated using a bash script (See S2 file). For average TPMs, arithmetic means of the TPMs for all replicates within a sample group were calculated in R along with the standard error.

Bead feeding assay

Adult worms were removed from the intestinal tract day 10 post-infection and isolated using a modified Baerman apparatus. They were washed three times with water and placed in Dulbecco's modified eagle's medium – high glucose (Sigma cat. D5796) where they were sexed and counted. Worms were either used immediately for feeding assays. Mixed sex groups of worms were incubated with or without beads ((108 beads per 5mL of media, Polysciences Inc., Cat. 18859-1for two days. Worms were euthanised with 70% ethanol. Images were acquired using the Zeiss Axio ZoomV.16 stereoscopic microscope (Bio Core Facility, Department of Biological Sciences, University of Calgary). Brightfield and fluorescence images were taken either under the the PlanNeoFluar Z 1x/0.25 FWD 56mm objective objective with the AxioCam High Resolution colour (HRc) and High-Resolution mono (HRm) cameras. Beads were counted manually by zooming into images by two independent observers.

References

1. Bethony JM, Cole RN, Guo X, Kamhawi S, Lightowlers MW, Loukas A, et al. Vaccines to combat the neglected tropical diseases. Immunol Rev. 2011;239: 237–270. doi:10.1111/j.1600-065X.2010.00976.x

2. Grisi L, Leite RC, Martins JR de S, de Barros ATM, Andreotti R, Cançado PHD, et al. Reassessment of the potential economic impact of cattle parasites in Brazil. Braz J Vet Parasitol. 2014;23: 150–156. doi:10.1590/S1984-29612014042

3. Stromberg BE, Gasbarre LC. Gastrointestinal Nematode Control Programs with an Emphasis on Cattle. Vet Clin Food Anim. 2006;22: 543–565. doi:10.1016/j.cvfa.2006.08.003

4. Smythe AB, Holovachov O, Kocot KM. Improved phylogenomic sampling of free-living nematodes enhances resolution of higher-level nematode phylogeny. BMC Evol Biol. 2019;19: 121–135. doi:10.1186/s12862-019-1444-x

5. Van Megen H, Van Den Elsen S, Holterman M, Karssen G, Mooyman P, Bongers T, et al. A phylogenetic tree of nematodes based on about 1200 full-length small subunit ribosomal DNA sequences. Nematology. 2009;11: 927–950. doi:10.1163/156854109X456862

6. Cable J, Harris PD, Lewis JW, Behnke JM. Molecular evidence that *Heligmosomoides polygyrus* from laboratory mice and wood mice are separate species. Parasitology. 2006;133: 111–122. doi:10.1017/S0031182006000047

7. Behnke J, Harris PD. *Heligmosomoides bakeri*: A new name for an old worm? Trends Parasitol. 2010;26: 524–529. doi:10.1016/j.pt.2010.07.001

587 8. Behnke JM, Keymer AE, Lewis JW. *Heligmosomoides polygyrus* or *Nematospiroides dubius*?
588 Parasitol Today. 1991;7: 177–179.

589 9. Bryant V. The life cycle of *Nematospiroides dubius*, Baylis, 1926 (Nematoda: Heligmosomidae). J
590 Helminthol. 1973;XLVII: 263–268.

591 10. Maizels RM, Hewitson JP, Murray J, Harcus YM, Dayer B, Filbey KJ, et al. Immune modulation and
592 modulators in *Heligmosomoides polygyrus* infection. Exp Parasitol. 2012;132: 76–89.
593 doi:10.1016/j.exppara.2011.08.011

594 11. Reynolds LA, Filbey KJ, Maizels RM. Immunity to the model intestinal helminth parasite
595 *Heligmosomoides polygyrus*. Semin Immunopathol. 2012;34: 829–846. doi:10.1007/s00281-012-
596 0347-3

597 12. International Helminth Genomes Consortium. Comparative genomics of the major parasitic
598 worms. Nat Genet. 2019;51: 163–174. doi:10.1038/s41588-018-0262-1

599 13. Chow FWN, Koutsovoulos G, Ovando-Vázquez C, Neophytou K, Bermúdez-Barrientos JR, Laetsch
600 DR, et al. Secretion of an Argonaute protein by a parasitic nematode and the evolution of its
601 siRNA guides. Nucleic Acids Res. 2019;47: 3594–3606. doi:10.1093/nar/gkz142

602 14. Rausch S, Midha A, Kuhring M, Affinass N, Radonic A, Kühl AA, et al. Parasitic nematodes exert
603 antimicrobial activity and benefit from microbiota-driven support for host immune regulation.
604 Front Immunol. 2018;9: 2282. doi:10.3389/fimmu.2018.02282

605 15. Buck AH, Coakley G, Simbari F, McSorley HJ, Quintana JF, Le Bihan T, et al. Exosomes secreted by
606 nematode parasites transfer small RNAs to mammalian cells and modulate innate immunity. Nat
607 Commun. 2014;5: 5488. doi:10.1038/ncomms6488

608 16. Maruszewska-Cheruiyot M, Szewczak L, Krawczak-Wójcik K, Głaczyńska M, Donskow-Łysoniewska
609 K. The production of excretory-secretory molecules from *Heligmosomoides polygyrus bakeri*
610 fourth stage larvae varies between mixed and single sex cultures. Parasites and Vectors. 2021;14:
611 106. doi:10.1186/s13071-021-04613-9

612 17. McNulty SN, Strübe C, Rosa BA, Martin JC, Tyagi R, Choi YJ, et al. *Dictyocaulus viviparus* genome,
613 variome and transcriptome elucidate lungworm biology and support future intervention. Sci Rep.
614 2016;6: 20316. doi:10.1038/srep20316

615 18. Jex AR, Nejsum P, Schwarz EM, Hu L, Young ND, Hall RS, et al. Genome and transcriptome of the
616 porcine whipworm *Trichuris suis*. Nat Genet. 2014;46: 701. doi:10.1038/ng.3012

617 19. Luck AN, Evans CC, Riggs MD, Foster JM, Moorhead AR, Slatko BE, et al. Concurrent
618 transcriptional profiling of *Dirofilaria immitis* and its *Wolbachia* endosymbiont throughout the
619 nematode life cycle reveals coordinated gene expression. BMC Genomics. 2014;15: 1041.
620 doi:10.1186/1471-2164-15-1041

621 20. Laing R, Kikuchi T, Martinelli A, Tsai IJ, Beech RN, Redman E, et al. The genome and transcriptome
622 of *Haemonchus contortus*, a key model parasite for drug and vaccine discovery. Genome Biol.
623 2013;14: R88. doi:10.1186/gb-2013-14-8-r88

624 21. MacKinnon BM. A light and electron microscopical investigation of fertilization, chromosome
625 behaviour, and early cleavage patterns in *Heligmosomoides polygyrus* (Nematoda:

626 Trichostrongyloidea). Int J Invertebr Reprod Dev. 1987;11: 89–108.

627 22. MacKinnon BM. An ultrastructural and histochemical study of oogenesis in the Trichostrongylid
628 Nematode *Heligmosomoides polygyrus*. J Parasitol. 1987;73: 390–399.

629 23. Miersch C, Döring F. Sex Differences in Carbohydrate Metabolism Are Linked to Gene Expression
630 in *Caenorhabditis elegans*. PLoS One. 2012;7: e44748. doi:10.1371/journal.pone.0044748

631 24. Reinke V, Gil IS, Ward S, Kazmer K. Genome-wide germline-enriched and sex-biased expression
632 profiles in *Caenorhabditis elegans*. Development. 2004;131: 311–323. doi:10.1242/dev.00914

633 25. Inoue H, Nishida E. The DM Domain Transcription Factor MAB-3 Regulates Male Hypersensitivity
634 to Oxidative Stress in *Caenorhabditis elegans*. Mol Cell Biol. 2010;30: 3453–3459.
635 doi:10.1128/mcb.01459-09

636 26. Ben-Smith A, Lammas DA, Behnke JM. Effect of oxygen radicals and differential expression of
637 catalase and superoxide dismutase in adult *Heligmosomoides polygyrus* during primary infections
638 in mice with differing response phenotypes. Parasite Immunol. 2002;24: 119–129.
639 doi:10.1046/j.1365-3024.2002.00445.x

640 27. Liu KS, Sternberg PW. Sensory regulation of male mating behavior in *Caenorhabditis elegans*.
641 Neuron. 1995;14: 79–89. doi:10.1016/0896-6273(95)90242-2

642 28. Gruninger TR, Gualberto DG, LeBoeuf B, Garcia LR. Integration of male mating and feeding
643 behaviors in *Caenorhabditis elegans*. J Neurosci. 2006;26: 169–179.
644 doi:10.1523/JNEUROSCI.3364-05.2006

645 29. Thoemke K, Yi W, Ross JM, Kim S, Reinke V, Zarkower D. Genome-wide analysis of sex-enriched
646 gene expression during *C. elegans* larval development. Dev Biol. 2005;284: 500–508.
647 doi:10.1016/j.ydbio.2005.05.017

648 30. Vanover-Dettling L, Komuniecki PR. Effect of gas phase on carbohydrate metabolism in *Ascaris*
649 *suum* larvae. Mol Biochem Parasitol. 1989;36: 29–39. doi:10.1016/0166-6851(89)90197-7

650 31. Roos MH, Tielens AGM. Differential expression of two succinate dehydrogenase subunit-B genes
651 and a transition in energy metabolism during the development of the parasitic nematode
652 *Haemonchus contortus*. Mol Biochem Parasitol. 1994;66: 273–281. doi:10.1016/0166-
653 6851(94)90154-6

654 32. Butler JA, Mishur RJ, Bokov AF, Hakala KW, Weintraub ST, Rea SL. Profiling the Anaerobic
655 Response of *C. elegans* Using GC-MS. PLoS One. 2012;7: e46140.
656 doi:10.1371/journal.pone.0046140

657 33. Kitazume H, Dayi M, Tanaka R, Kikuchi T. Assessment of the behaviour and survival of nematodes
658 under low oxygen concentrations. PLoS One. 2018;13: e0197122.
659 doi:10.1371/journal.pone.0197122

660 34. Zheng L, Kelly CJ, Colgan SP. Physiologic hypoxia and oxygen homeostasis in the healthy intestine.
661 A review in the theme: Cellular responses to hypoxia. Am J Physiol Cell Physiol. 2015;309: C350–
662 C360. doi:10.1152/ajpcell.00191.2015

663 35. Page AP, Stepek G, Winter AD, Pertab D. Enzymology of the nematode cuticle: A potential drug

target? Int J Parasitol Drugs Drug Resist. 2014;4: 133–141. doi:10.1016/j.ijpddr.2014.05.003

36. Myllyharju J. Prolyl 4-hydroxylases, key enzymes in the synthesis of collagens and regulation of the response to hypoxia, and their roles as treatment targets. Ann Med. 2008;40: 402–417. doi:10.1080/07853890801986594

37. Rodrigues RR, Gennari SM, Guerra JL, Contieri MB, Abdalla AL, Vitti DMSS. Histopathological changes during experimental infections of calves with *Cooperia punctata*. J Helminthol. 2004;78: 167–171. doi:10.1079/joh2003217

38. Bruschi F, Ashour DS, Othman AA. *Trichinella*-induced immunomodulation: Another tale of helminth success. Food Waterborne Parasitol. 2022;27: e00164. doi:10.1016/j.fawpar.2022.e00164

39. Else KJ, Keiser J, Holland C V., Grencis RK, Sattelle DB, Fujiwara RT, et al. Whipworm and roundworm infections. Nat Rev Dis Prim. 2020;6: 44. doi:10.1038/s41572-020-0171-3

40. Loukas A, Prociv P. Immune responses in hookworm infections. Clin Microbiol Rev. 2001;14: 689–703. doi:10.1128/CMR.14.4.689-703.2001

41. Montaño KJ, Cuéllar C, Sotillo J. Rodent Models for the Study of Soil-Transmitted Helminths: A Proteomics Approach. Front Cell Infect Microbiol. 2021;11: 639573. doi:10.3389/fcimb.2021.639573

42. Besier RB, Kahn LP, Sargison ND, Van Wyk JA. The Pathophysiology, Ecology and Epidemiology of *Haemonchus contortus* Infection in Small Ruminants. Advances in Parasitology. Elsevier Ltd; 2016. doi:10.1016/bs.apar.2016.02.022

43. Uno M, Nishida E. Lifespan-regulating genes in *C. elegans*. npj Aging Mech Dis. 2016;2: 16010. doi:10.1038/npjamd.2016.10

44. Hotzi B, Kosztelnik M, Hargitai B, Takács-Vellai K, Barna J, Bördén K, et al. Sex-specific regulation of aging in *Caenorhabditis elegans*. Aging Cell. 2018;17: e12724. doi:10.1111/acel.12724

45. Froehlich JJ, Rajewsky N, Ewald CY. Estimation of *C. elegans* cell- and tissue volumes. microPublication Biol. 2021. doi:10.17912/micropub.biology.000345

46. Chehayeb JF, Robertson AP, Martin RJ, Geary TG. Proteomic Analysis of Adult *Ascaris suum* Fluid Compartments and Secretory Products. PLoS Negl Trop Dis. 2014;8: e2939. doi:10.1371/journal.pntd.0002939

47. Smyth DJ, Harcus Y, White MPJ, Gregory WF, Nahler J, Stephens I, et al. TGF- b mimic proteins form an extended gene family in the murine parasite *Heligmosomoides polygyrus*. Int J Parasitol. 2018;48: 379–385. doi:10.1016/j.ijpara.2017.12.004

48. Osbourn M, Soares DC, Vacca F, Cohen ES, Scott IC, Gregory WF, et al. HpARI Protein Secreted by a Helminth Parasite Suppresses Interleukin-33. Immunity. 2017;47: 739–751. doi:10.1016/j.immuni.2017.09.015

49. Humphreys NE, Xu D, Hepworth MR, Liew FY, Grencis RK. IL-33, a Potent Inducer of Adaptive Immunity to Intestinal Nematodes. J Immunol. 2008;180: 2443–2449. doi:10.4049/jimmunol.180.4.2443

50. Pollo SMJ, Adebusuyi AA, Straub TJ, Foght JM, Zhaxybayeva O, Nesbø CL. Genomic insights into temperature-dependent transcriptional responses of Kosmotoga olearia, a deep-biosphere bacterium that can grow from 20 to 79 °C. Extremophiles. 2017;21: 963–979. doi:10.1007/s00792-017-0956-9

51. Dobin A, Davis CA, Schlesinger F, Drenkow J, Zaleski C, Jha S, et al. STAR: Ultrafast universal RNA-seq aligner. Bioinformatics. 2013;29: 15–21. doi:10.1093/bioinformatics/bts635

52. Liao Y, Smyth GK, Shi W. featureCounts: An efficient general purpose program for assigning sequence reads to genomic features. Bioinformatics. 2014;30: 923–930. doi:10.1093/bioinformatics/btt656

53. Love MI, Huber W, Anders S. Moderated estimation of fold change and dispersion for RNA-seq data with DESeq2. Genome Biol. 2014;15: 550. doi:10.1186/s13059-014-0550-8

54. Russo PST, Ferreira GR, Cardozo LE, Bürger MC, Arias-Carrasco R, Maruyama SR, et al. CEMiTool: A Bioconductor package for performing comprehensive modular co-expression analyses. BMC Bioinformatics. 2018;19: 56. doi:10.1186/s12859-018-2053-1

55. Kolberg L, Raudvere U, Kuzmin I, Vilo J, Peterson H. gprofiler2 -- an R package for gene list functional enrichment analysis and namespace conversion toolset g: Profiler. F1000Research. 2020;9: ELIXIR-709. doi:10.12688/f1000research.24956.2

56. Wolstenholme AJ. Ion channels and receptor as targets for the control of parasitic nematodes. Int J Parasitol Drugs Drug Resist. 2011;1: 2–13. doi:10.1016/j.ijpddr.2011.09.003

57. Atkinson LE, McCoy CJ, Crooks BA, McKay FM, McVeigh P, McKenzie D, et al. Phylum-Spanning Neuropeptide GPCR Identification and Prioritization: Shaping Drug Target Discovery Pipelines for Nematode Parasite Control. Front Endocrinol (Lausanne). 2021;12: 718363. doi:10.3389/fendo.2021.718363

Supporting Information

S1 Text. Supplementary Results and Discussion.

S1 Fig. Principal component biplots of the RNA-seq datasets used in this study. A) Biplot of the first two components from the PCA of the raw counts. B) Biplot of the first two components from the PCA of the VST-transformed counts.

S2 Fig. Hierarchical clustering dendrograms of the datasets used in this study. A) HC using Euclidean distance and average linkage. B) HC using Manhattan distance and average linkage. C) HC using Canberra distance and average linkage.

S3 Fig. Transcript co-expression networks. Normalized enrichment scores, reflecting the expression values of the genes in the module, are plotted for each module returned by the network. Unsigned networks allow strong negative correlations to be connected within a module, whereas signed networks do not. Both are shown.

S4 Fig. Expression of orthologs of genes in *C. elegans* that have been implicated in aging. Scatterplots of the VST-transformed read counts (which estimate expression level of the transcript) for all samples grouped by their age/sex combination. The transcript in *H. bakeri* and ortholog in *C. elegans* are shown above the plot.

S5 Fig. Expression of immunomodulatory genes. The arithmetic mean for each age/sex group of the VST-transformed read counts (which estimate expression level of the transcript) are plotted for every transcript matching the description above each plot. Average expression values for female samples are on the left and transcripts are plotted with an open circle connected by lines. Average expression values for male samples are on the right and transcripts are plotted with closed squares connected by lines. Symbols and lines are colour coded to indicate the transcript being plotted with each being labelled in the legend to the right of the plot.

S1 File. Supplementary Tables.xlsx. All Supplementary Tables referenced in the main text.

S2 File. Compressed file of Linux and R commands used in all analyses.

S3 File. Readcountmatrix_fcssall.xlsx. Matrix of read counts per transcript for all RNA-seq datasets included in this study.

S4 File. Compressed file of all the images used for the bead-feeding assay.

Figure Captions

Fig 1. Life cycle of *H. bakeri*. Eggs present in mouse feces develop through two larval stages and arrest during their infective L3 stage. Upon being eaten by a mouse host the L3s exsheath in the stomach and upper duodenum and burrow into the duodenum tissue to form a granuloma. Development continues until the final molt to the adult form when the worms migrate to the lumen of the duodenum where they mate and lay their eggs that get passed with the feces.

Fig 2. Numbers of transcripts statistically significantly up- and down-regulated in sample group comparisons. Numbers are positioned and coloured according to the comparison being described. Purple center: transcripts up-regulated (top number beside up arrow) or down-regulated (bottom number beside down arrow) in females vs. males at the age to the left, green: transcripts up- or down-regulated in D5 vs D7 females (left) or males (right), orange: transcripts up- or down-regulated in D7 vs D10 females or males, blue: transcripts up- or down-regulated in D10 vs D21 females or males, black: transcripts up-regulated in all female (URF) or male (URM) samples at all ages, red: tissue-dwelling vs lumen-dwelling comparisons (up: URTDF, URTDM; down: URLDF, URLDM).

Fig 3. Flow diagram of male/female comparisons. The intersections of pairwise comparisons between age-matched male and female samples were filtered to yield the sets of transcripts discussed in the main text.

Fig 4. Comparison between the feeding of female and male D10 adults, both n=14. (A) The number of beads ingested normalised for the worms' size difference. There was not a significant difference between the sexes (p=0.06), but the females and males were differently distributed. Only females

775 ingested beads at the higher rate (circle). (B) Representative pictures of a female and male D10 worms.
776 All the images are available in the S4 File.

777 Fig 5. Volcano plots of male / female comparisons at D5 (A), D7 (B), D10 (C), and D21 (D). The transcripts
778 in URM (blue) or URF (green) are shown. Negative log2FoldChanges denote higher expression in the
779 male group while positive values indicate higher expression in the female group. Marker genes in red
780 are 1) *her-1* (HPOL_0000740701), 2) *mab-3* (HPOL_0001902701), 3) *spe-4* (HPOL_0000308001), 4) *csn-1*
781 (HPOL_0001830501), 5) *fox-1* (HPOL_0001264601), and 6) *perm-4* (HPOL_0000100601).

782 Fig 6. Flow diagram of developmental comparisons. Transcripts with expression patterns of interest
783 were filtered according to co-expression network module and statistically significant differences in
784 expression in pairwise comparisons between tissue-dwelling and lumen-dwelling worms to yield the sets
785 of transcripts discussed in the main text.

786 Fig 7. Expression in *H. bakeri* of orthologs of genes in *C. elegans* implicated in aging. Average TPM
787 (transcript per million) are plotted for females (left) and males (right) at each timepoint. Error bars
788 represent standard error. The insulin receptor (*daf-2*), kinase (*age-1*), and *daf-16/FOXO* transcription
789 factor (*daf-16*) of the IIS pathway are shown along with the master energy regulator (*aak-2*).

790 Fig 8. Expression of immunomodulatory genes in male and female *H. bakeri*. Average TPM (transcript
791 per million) are plotted for females (left) and males (right) at each timepoint. Error bars represent
792 standard error. The only identified immunomodulatory genes to date are plotted: HbARI (top row),
793 HbBARI and HbBARI_Hom2(middle row), and HbTGM-6 (bottom row).

794 Fig 9. Schematic of the HbARI locus highlighting that the annotations in *H. bakeri* still need work. The
795 two genome assemblies for *H. bakeri*, PRJEB1203 and PRJEB15396 (shown collectively as a black line),
796 agree in this region with the exception of the area shown in the black box. The conflicting annotations
797 for HbARI, HPBE_0000813301 (teal) and HPOL_0001636401 (green), are shown in their annotated
798 positions and drawn to scale. HPOL_0001636401 is shorter at the 5' end and consequently does not
799 contain the signal peptide predicted to be in HPBE_0000813301. Since we know HbARI is a secreted
800 protein because it was identified among HES, the PRJEB15396 annotation must be incorrect. As it is,
801 HPOL_0001636401 is predicted to localize to the mitochondrion (data not shown). The coverage of all of
802 the RNA-seq reads generated in this study in this region is shown as a line graph above the annotations.
803 The HPBE_0000813301 annotation contains an extra 5' exon that has no support in any of the RNA-seq
804 datasets.

805

806

807 **Tables**

808 Table 1. Metadata of the RNA-seq samples in this study.

Sample Name	File Name	# worms extracted	Days Post Infection	RIN	Reads Uniquely Mapped / Total Reads (%)	Included in Pairwise Comparisons?
D5 F2	D5-F2_Li29408_S5	174	5	9.6	112169129 / 118520168 (94.64)	Yes

D5 F3	D5-F3_Li29409_S6	297	5	9.4	129241490 / 136943707 (94.38)	Yes
D5 F4	D5-F4_Li29410_S7	173	5	9.3	107651456 / 113590373 (94.77)	Yes
D5 F5	D5-F5_Li29411_S8	232	5	9.5	118950175 / 125198338 (95.01)	Yes
D5 M1	D5-M1_Li29404_S1	132	5	9.3	128308873 / 135898387 (94.42)	Yes
D5 M2	D5-M2_Li29405_S2	100	5	9.5	124417881 / 131400648 (94.69)	Yes
D5 M4	D5-M4_Li29406_S3	95	5	9.6	138697190 / 146832868 (94.46)	Yes
D5 M5	D5-M5_Li29407_S4	179	5	9.6	134892659 / 142089783 (94.93)	Yes
D7 F1	D7-F1_Li29416_S13	150	7	9.4	108668904 / 114523342 (94.89)	Yes
D7 F4	D7-F4_Li29417_S14	211	7	9.2	141571706 / 149554981 (94.66)	Yes
D7 F5	D7-F5_Li29418_S15	120	7	9.4	131197468 / 138924573 (94.44)	Yes
D7 F6	D7-F6_Li29419_S16	205	7	9.4	144299969 / 153229819 (94.17)	Yes
D7 M1	D7-M1_Li29412_S9	126	7	9.5	135646150 / 143790919 (94.34)	Yes
D7 M2	D7-M2_Li29413_S10	89	7	9.3	138636801 / 147210080 (94.18)	Yes
D7 M4	D7-M4_Li29414_S11	144	7	9.6	113177165 / 119922840 (94.37)	Yes
D7 M7	D7-M7_Li29415_S12	85	7	9.7	117210623 / 124680285 (94.01)	Yes
D10 F1	D10-F1_Li29424_S21	100	10	9.6	126048861 / 132664380 (95.01)	Yes
D10 F2	D10-F2_Li29425_S22	100	10	9.9	117253862 / 123536616 (94.91)	Yes
D10 F6	D10-F6_Li29426_S23	80	10	9.7	128203029 / 136497304 (93.92)	No
D10 F7	D10-F7_Li29427_S24	80	10	9.8	130193841 / 138092543 (94.28)	No
D10 F8	D10-F8_Li31315_S1	80	10	9.4	166132630 / 173733692 (95.62)	Yes
D10 F9	D10-F9_Li31316_S2	80	10	9.2	196647784 / 205996448 (95.46)	Yes
D10 F10	D10-F10_Li31317_S3	80	10	9.3	170031664 / 178491143 (95.26)	Yes
D10 F11	D10-F11_Li31318_S4	80	10	9.2	162920697 / 170951647 (95.30)	Yes
D10 F13	D10-F13_Li31319_S5	80	10	9.5	147832599 / 155432294 (95.11)	Yes
D10 M1	D10-M1_Li29420_S17	100	10	9.4	135805443 / 145141041 (93.57)	Yes
D10 M2	D10-M2_Li29421_S18	100	10	9.6	128421348 / 137123098 (93.65)	Yes
D10 M3	D10-M3_Li29422_S19	80	10	9.5	130675067 / 138649879 (94.25)	Yes
D10 M6	D10-M6_Li29423_S20	80	10	9.8	110098546 / 116957271 (94.14)	Yes
D21 F5	D21-F5_Li29432_S29	80	21	9.1	108798485 / 114364046 (95.13)	Yes
D21 F6	D21-F6_Li29433_S30	80	21	9.5	100100633 / 104891911 (95.43)	Yes
D21 F11	D21-F11_Li29434_S31	80	21	9.4	98844233 / 103850834 (95.18)	Yes
D21 F12	D21-F12_Li29435_S32	80	21	4.9	100561928 / 105898940 (94.96)	Yes
D21 M5	D21-M5_Li29428_S25	80	21	9	114067372 / 122106224 (93.42)	Yes
D21 M7	D21-M7_Li29429_S26	80	21	8.7	122812424 / 131448504 (93.43)	Yes
D21 M12	D21-M12_Li29430_S27	80	21	9.2	122775218 / 130863303 (93.82)	Yes
D21 M13	D21-M13_Li29431_S28	80	21	9.1	104773522 / 112342173 (93.26)	Yes

Table 2. Expression of immunomodulatory genes in *H. bakeri*.

Protein Name	**HbARI**	**HbBARI**	**HbBARI_Hom2**	**Hb-TGM-6**

H. bakeri **Locus Tag**	**HPOL_0001636401**	**HPOL_0001228301**	**HPOL_0001228401**	**HPOL_0001864701**
D5 Male Average TPM	1157.52	85.66	2189.10	11.08
D5 Male vs D7 Male padj	2.78E-01	1.81E-01	2.79E-25	1.14E-06
D7 Male Average TPM	1137.80	71.52	599.96	47.05
D7 Male vs D10 Male padj	3.91E-43	6.40E-01	2.18E-212	1.26E-02
D10 Male Average TPM	145.43	53.57	5.80	63.04
D10 Male vs D21 Male padj	1.48E-01	2.35E-07	9.88E-39	6.78E-01
D21 Male Average TPM	201.43	217.55	0.65	87.04
D5 Female Average TPM	1052.13	228.89	2097.85	16.25
D5 Female vs D7 Female padj	2.91E-01	9.60E-01	2.56E-08	5.92E-03
D7 Female Average TPM	1070.11	202.22	824.01	30.71
D7 Female vs D10 Female padj	1.65E-174	2.62E-07	0.00E+00	1.85E-03
D10 Female Average TPM	64.18	85.79	7.71	17.48
D10 Female vs D21 Female padj	7.07E-01	1.07E-01	4.38E-41	3.62E-01
D21 Female Average TPM	63.68	140.27	0.06	13.54

812

Table 3. Expression of drug targets in male *H. bakeri*. Values in bold are padj < 0.05.

Drug class	Target	*C. elegans* gene	*H. bakeri* PRJEB15396 Gene	D5 Male Average TPM	D5 Male vs D7 Male padj	D7 Male Average TPM	D7 Male vs D10 Male padj	D10 Male Average TPM	D10 Male vs D21 Male padj	D21 Male Average TPM
Macrocyclic lactones	GluCl	*glc-1*	HPOL_0001177601-mRNA-1	3.91	**3.06E-09**	8.84	**1.24E-02**	4.52	**1.03E-04**	2.74
		glc-2	HPOL_0001003101-mRNA-1	1.32	7.05E-01	1.62	3.71E-01	1.33	3.69E-01	1.75
			HPOL_0001839701-mRNA-1	0.60	5.95E-02	0.93	4.26E-01	0.56	1.94E-01	0.79
		glc-3	HPOL_0000126101-mRNA-1	2.03	**4.84E-09**	1.34	**2.92E-04**	0.64	2.52E-01	0.80
		avr-14	HPOL_0000096601-mRNA-1	1.67	**5.20E-07**	0.93	2.84E-01	0.55	2.89E-01	0.73
		avr-15	HPOL_0001177601-mRNA-1	3.91	**3.06E-09**	8.84	**1.24E-02**	4.52	**1.03E-04**	2.74
Piperazine	GABA	*unc-49*	HPOL_0000247101-mRNA-1	7.52	**2.81E-07**	5.06	6.81E-01	3.31	**2.35E-02**	4.74
Imidazothiazoles, tetrahydropyrimidine, tribendimidine, spiroindoles	nACHR	*lev-1*	HPOL_0001059501-mRNA-1	9.09	**2.15E-13**	4.73	**5.22E-03**	2.31	**8.67E-04**	3.91
		lev-8	HPOL_0000812201-mRNA-1	0.21	1.40E-01	0.14	**3.13E-04**	0.39	**2.72E-03**	0.10
		unc-29	HPOL_0000079901-mRNA-1	19.38	**1.25E-13**	12.55	2.39E-01	7.86	1.47E-01	9.66
			HPOL_0001278501-mRNA-1	1.83	**1.56E-06**	1.06	2.62E-01	0.62	9.41E-01	0.61
			HPOL_0001278801-mRNA-1	0.16	2.73E-01	0.29	6.50E-02	0.08	NA	0.11
			HPOL_0002208401-mRNA-1	0.12	8.02E-01	0.12	9.95E-01	0.09	NA	0.16
			HPOL_0000080001-mRNA-1	9.12	**5.53E-48**	1.75	**4.33E-04**	1.89	7.59E-01	1.84
		unc-38	HPOL_0000053201-mRNA-1	19.64	**2.05E-12**	12.28	1.04E-01	7.34	9.81E-01	7.67
		unc-63	HPOL_0000939601-mRNA-1	6.62	**8.10E-03**	6.07	2.48E-01	3.91	7.38E-02	3.25
AADs	Cholinerecptors	*acr-23*	HPOL_0000939601-mRNA-1	6.62	**8.10E-03**	6.07	2.48E-01	3.91	7.38E-02	3.25
		deg-3	HPOL_0000510801-mRNA-1	2.00	**3.97E-04**	1.58	8.63E-02	0.92	1.12E-01	1.19
		des-2	HPOL_0000510601-mRNA-1	3.22	**2.36E-02**	2.88	1.90E-01	1.75	1.71E-01	2.23
			HPOL_0000510701-mRNA-1	5.27	**6.61E-04**	4.19	3.59E-01	2.64	5.60E-01	3.05
Cyclic depsipeptides	Potassium channels	*slo-1*	HPOL_0000350101-mRNA-1	14.86	**5.42E-04**	22.46	**3.73E-05**	22.22	**8.57E-03**	17.53

Cyclic depsipeptides	Latrophilin receptors	*lat-1*	HPOL_0001283901-mRNA-1	31.93	4.06E-01	32.41	2.28E-01	19.90	8.21E-01	18.55
Benzimidazole	TBBs	*ben-1*	HPOL_0000661601-mRNA-1	1243.07	**8.60E-07**	1025.66	**9.86E-08**	1004.27	4.10E-01	966.08
			HPOL_0000662001-mRNA-1	343.07	**5.49E-61**	140.36	**2.06E-02**	84.42	**1.12E-03**	67.44
Of interest**	neuropeptide GPCRs	*pdfr-1*	HPOL_0000292001-mRNA-1	2.36	**5.83E-04**	1.35	3.85E-01	1.25	1.39E-01	0.77
		pcdr-1	HPOL_0000775801-mRNA-1	18.52	**7.19E-07**	13.93	**8.18E-06**	14.11	4.57E-01	13.29
		npr-11	HPOL_0001846201-mRNA-1	1.70	9.22E-01	1.96	**1.13E-02**	1.80	3.93E-01	1.63
		fshr-1	HPOL_0000573301-mRNA-1	8.24	6.14E-01	8.85	**1.91E-03**	4.57	9.84E-02	3.81
			HPOL_0000675901-mRNA-1	6.95	4.02E-01	6.88	8.55E-02	3.70	8.81E-01	3.65
		npr-5	HPOL_0000717801-mRNA-1	24.43	**6.72E-06**	17.02	8.11E-02	9.90	**3.20E-02**	13.66
		npr-4	HPOL_0000350501-mRNA-1	1.92	**3.17E-04**	1.40	**5.82E-16**	0.30	1.04E-01	0.46
		npr-10								
		npr-8								
		npr-9								
		frpr-7	HPOL_0000332701-mRNA-1	1.02	7.52E-01	1.26	**1.72E-02**	0.48	7.84E-01	0.60
			HPOL_0001927801-mRNA-1	0.45	7.14E-01	0.55	**1.94E-02**	0.23	8.00E-01	0.27
		frpr-18	HPOL_0002147401-mRNA-1	1.16	7.19E-01	1.39	5.30E-01	0.89	9.96E-01	0.93
			HPOL_0002202601-mRNA-1	0.50	2.10E-01	0.73	1.61E-01	0.66	6.34E-01	0.59
			HPOL_0002243501-mRNA-1	0.11	4.07E-01	0.19	3.40E-01	0.20	3.44E-01	0.11
		dmsr-1	HPOL_0001923201-mRNA-1	8.73	4.44E-01	10.74	**2.60E-04**	5.43	**8.92E-03**	7.48
		daf-38								
		dmsr-7	HPOL_0000318201-mRNA-1	4.13	5.95E-01	5.81	**2.23E-02**	1.82	9.52E-01	2.09
		frpr-5	HPOL_0000014001-mRNA-1	236.59	**1.51E-03**	183.85	**1.30E-05**	210.49	6.68E-01	203.18
		frpr-19	HPOL_0000877201-mRNA-1	27.56	**9.51E-10**	16.61	**5.37E-07**	6.86	1.98E-01	8.58
		gnrr-1	HPOL_0000032901-mRNA-1	1.33	5.26E-02	0.90	**7.58E-07**	2.51	8.04E-02	1.27
		sprr-1	HPOL_0000343501-mRNA-1	0.67	**3.01E-02**	0.51	8.15E-02	0.25	9.86E-01	0.27
		ckr-2								

		npr-16								
		frpr-9	HPOL_0001450601-mRNA-1	3.79	5.57E-01	5.08	2.80E-01	5.31	8.48E-02	2.77

**Atkinson et al., 2021

Table 4. Expression of drug targets in female *H. bakeri*. Values in bold are padj < 0.05.

Drug class	Target	*C. elegans* gene	*H. bakeri* PRJEB15396 Gene	D5 Female Average TPM	D5 Female vs D7 Female padj	D7 Female Average TPM	D7 Female vs D10 Female padj	D10 Female Average TPM	D10 Female vs D21 Female padj	D21 Female Average TPM
Macrocyclic lactones	GluCl	*glc-1*	HPOL_0001177601-mRNA-1	2.55	3.14E-01	2.56	**4.27E-112**	0.26	8.09E-01	0.28
		glc-2	HPOL_0001003101-mRNA-1	1.53	2.35E-01	1.66	**1.54E-09**	0.85	**9.28E-04**	1.58
			HPOL_0001839701-mRNA-1	0.96	4.64E-01	0.96	**4.88E-10**	0.49	6.14E-01	0.60
		glc-3	HPOL_0000126101-mRNA-1	2.43	**2.45E-02**	1.68	**3.84E-59**	0.49	9.32E-01	0.53
		avr-14	HPOL_0000096601-mRNA-1	1.28	**3.64E-02**	0.80	**1.45E-16**	2.62	9.90E-01	2.77
		avr-15	HPOL_0001177601-mRNA-1	2.55	3.14E-01	2.56	**4.27E-112**	0.26	8.09E-01	0.28
Piperazine	GABA	*unc-49*	HPOL_0000247101-mRNA-1	9.40	**1.13E-03**	5.78	**3.95E-38**	2.04	**2.32E-03**	3.18
Imidazothiazoles, tetrahydropyrimidine, tribendimidine, spiroindoles	nACHR	*lev-1*	HPOL_0001059501-mRNA-1	9.90	**1.59E-05**	5.35	**3.15E-57**	1.27	1.61E-01	1.69
		lev-8	HPOL_0000812201-mRNA-1	0.10	**3.17E-11**	0.86	**4.40E-09**	4.97	9.96E-01	5.25
		unc-29	HPOL_0000079901-mRNA-1	19.00	1.58E-01	14.56	**5.55E-98**	4.17	1.89E-01	3.88
			HPOL_0001278501-mRNA-1	1.67	7.87E-02	1.11	**9.81E-39**	0.23	5.16E-01	0.20
			HPOL_0001278801-mRNA-1	0.17	7.20E-02	0.05	**1.16E-02**	0.01	NA	0.01
			HPOL_0002208401-mRNA-1	0.19	5.18E-01	0.11	**3.23E-04**	0.01	NA	0.02
			HPOL_0000080001-mRNA-1	3.99	**1.08E-10**	1.52	**5.56E-05**	1.13	**1.48E-08**	0.54
		unc-38	HPOL_0000053201-mRNA-1	22.93	**7.43E-11**	11.33	**5.47E-92**	2.89	6.94E-01	3.23
		unc-63	HPOL_0000939601-mRNA-1	7.12	2.38E-01	6.90	**2.04E-37**	19.16	**2.59E-06**	28.98
AADs	Choline receptors	*acr-23*	HPOL_0000939601-mRNA-1	7.12	2.38E-01	6.90	**2.04E-37**	19.16	**2.59E-06**	28.98
		deg-3	HPOL_0000510801-mRNA-1	2.88	**7.91E-22**	0.93	**3.38E-65**	0.16	**1.99E-03**	0.29
		des-2	HPOL_0000510601-mRNA-1	4.79	**2.50E-15**	1.86	**3.84E-63**	0.35	**3.69E-02**	0.54
			HPOL_0000510701-mRNA-1	7.38	**2.99E-18**	2.61	**1.21E-66**	0.51	8.04E-01	0.58

Cyclic depsipeptides	Potassium channels	*slo-1*	HPOL_0000350101-mRNA-1	7.88	**3.13E-05**	9.75	**2.17E-81**	43.43	**3.15E-10**	28.62
Cyclic depsipeptides	Latrophilin receptors	*lat-1*	HPOL_0001283901-mRNA-1	37.69	**8.75E-04**	50.16	**6.33E-03**	79.58	8.40E-01	81.43
Benzimidazole	TBBs	*ben-1*	HPOL_0000661601-mRNA-1	1321.16	**1.68E-20**	632.90	**4.77E-08**	1014.55	9.91E-01	1077.80
			HPOL_0000662001-mRNA-1	280.90	8.85E-01	240.71	**8.45E-04**	342.77	9.67E-01	365.69
Of interest**	neuropeptide GPCRs	*pdfr-1*	HPOL_0000292001-mRNA-1	2.80	8.30E-01	2.58	**1.72E-15**	11.73	9.17E-01	12.89
		pcdr-1	HPOL_0000775801-mRNA-1	15.63	7.88E-01	14.02	**3.28E-08**	24.64	**2.19E-02**	32.22
		npr-11	HPOL_0001846201-mRNA-1	2.12	**1.23E-18**	4.64	**8.17E-79**	0.98	5.33E-01	0.93
		fshr-1	HPOL_0000573301-mRNA-1	13.07	7.91E-01	10.97	**1.81E-08**	8.27	8.60E-01	8.55
			HPOL_0000675901-mRNA-1	12.42	2.48E-01	8.96	**5.23E-12**	4.74	7.47E-01	5.38
		npr-5	HPOL_0000717801-mRNA-1	25.61	**3.44E-06**	13.28	2.59E-01	17.56	6.37E-01	20.15
		npr-4	HPOL_0000350501-mRNA-1	1.36	7.05E-01	1.26	**1.11E-29**	0.40	**5.48E-03**	0.26
		npr-10								
		npr-8								
		npr-9								
		frpr-7	HPOL_0000332701-mRNA-1	1.83	5.45E-02	1.01	**9.75E-12**	0.30	4.69E-01	0.42
			HPOL_0001927801-mRNA-1	0.92	1.79E-01	0.58	**1.09E-10**	0.20	7.28E-01	0.19
		frpr-18	HPOL_0002147401-mRNA-1	1.45	4.02E-01	1.42	**5.12E-10**	0.88	**7.03E-06**	0.49
			HPOL_0002202601-mRNA-1	0.68	3.84E-01	0.71	**2.47E-05**	0.43	**6.38E-03**	0.23
			HPOL_0002243501-mRNA-1	0.17	2.81E-01	0.25	**1.66E-04**	0.07	1.95E-01	0.02
		dmsr-1	HPOL_0001923201-mRNA-1	13.94	9.97E-01	12.08	**5.47E-140**	1.99	**2.88E-02**	2.67
		daf-38								
		dmsr-7	HPOL_0000318201-mRNA-1	4.97	8.99E-01	4.07	**4.20E-08**	1.05	9.91E-01	1.11
		frpr-5	HPOL_0000014001-mRNA-1	281.27	7.71E-02	308.84	**3.76E-16**	159.23	**4.37E-02**	129.39
		frpr-19	HPOL_0000877201-mRNA-1	28.02	**1.19E-06**	14.43	**4.71E-29**	6.12	6.33E-02	8.20
		gnrr-1	HPOL_0000032901-mRNA-1	1.05	**2.54E-03**	2.05	**1.07E-29**	27.44	9.68E-01	28.57

		sprr-1	HPOL_0000343501-mRNA-1	0.76	5.69E-01	0.58	**7.87E-18**	0.16	9.41E-02	0.10
		ckr-2								
		npr-16								
		frpr-9	HPOL_0001450601-mRNA-1	2.78	**1.21E-06**	8.13	**4.34E-16**	52.54	6.94E-01	64.31

**Atkinson et al., 2021

Figure 1

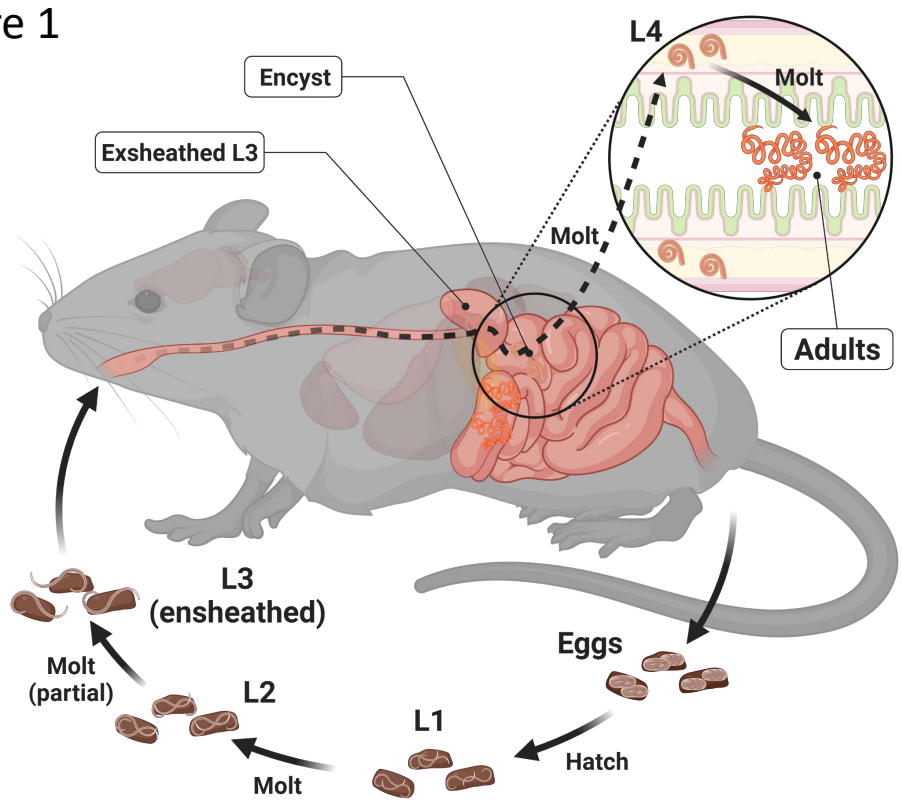

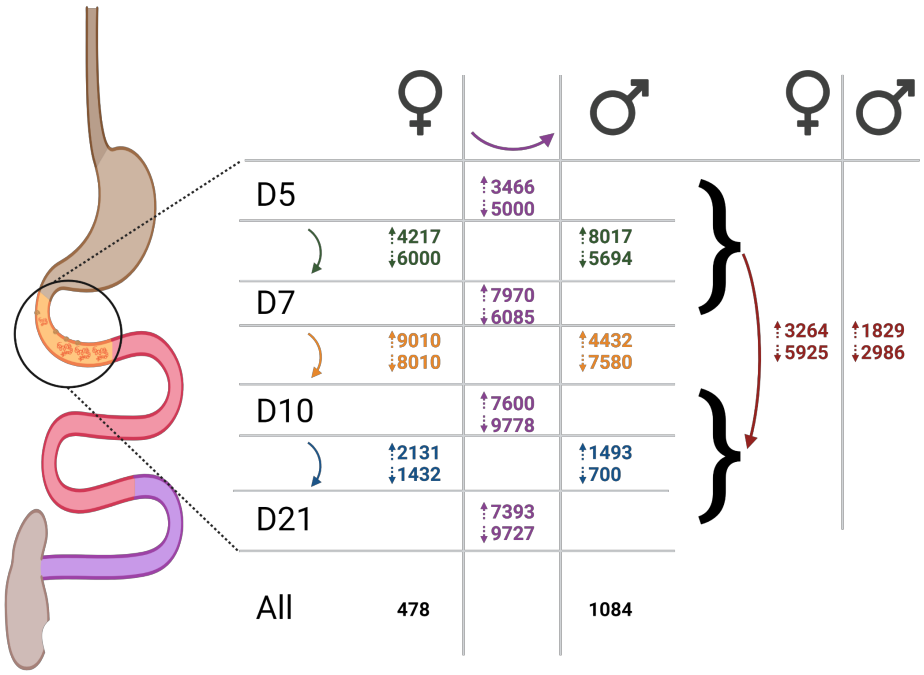

Figure 2

Figure 3

Transcriptional differences in males and females:

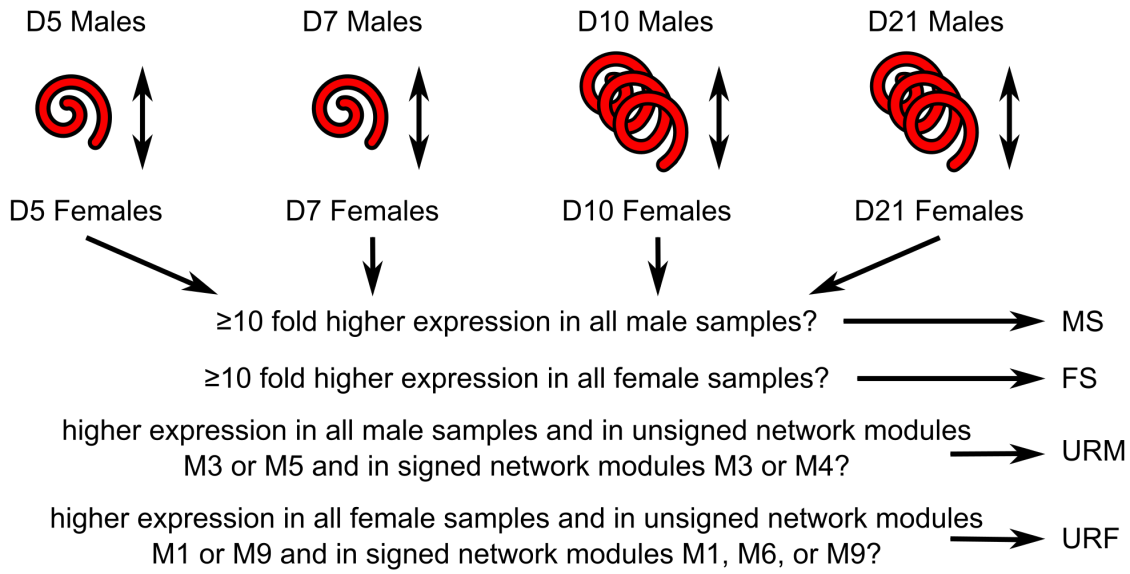

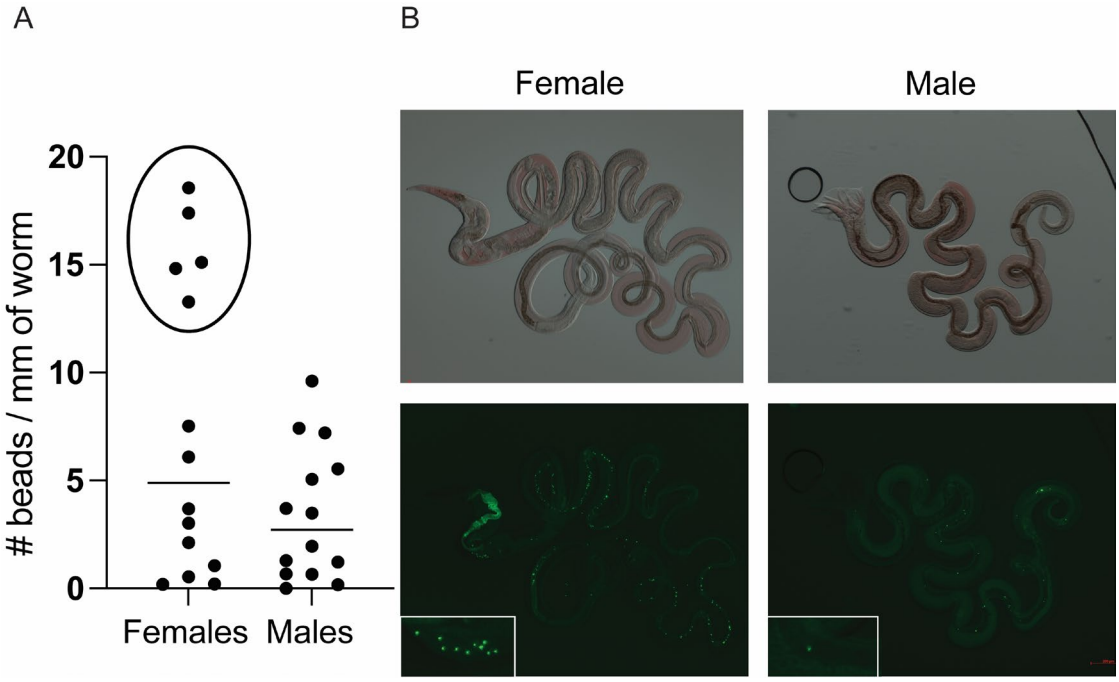

Figure 4

Figure 5

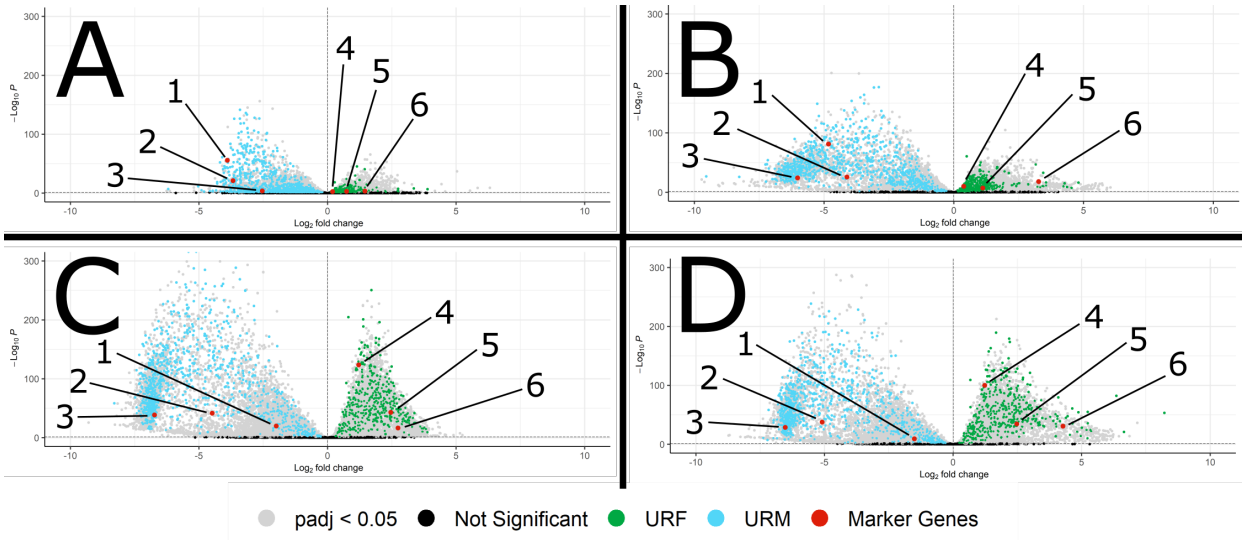

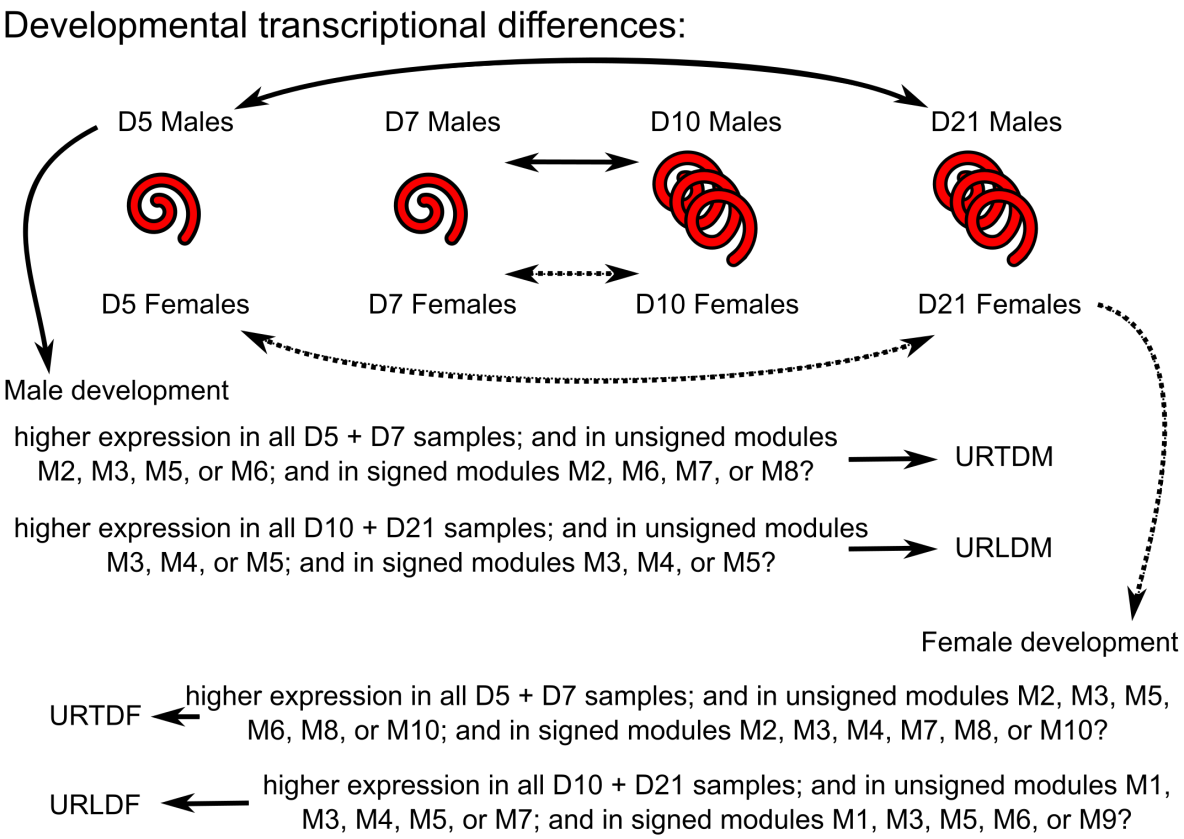

Figure 6

Figure 7

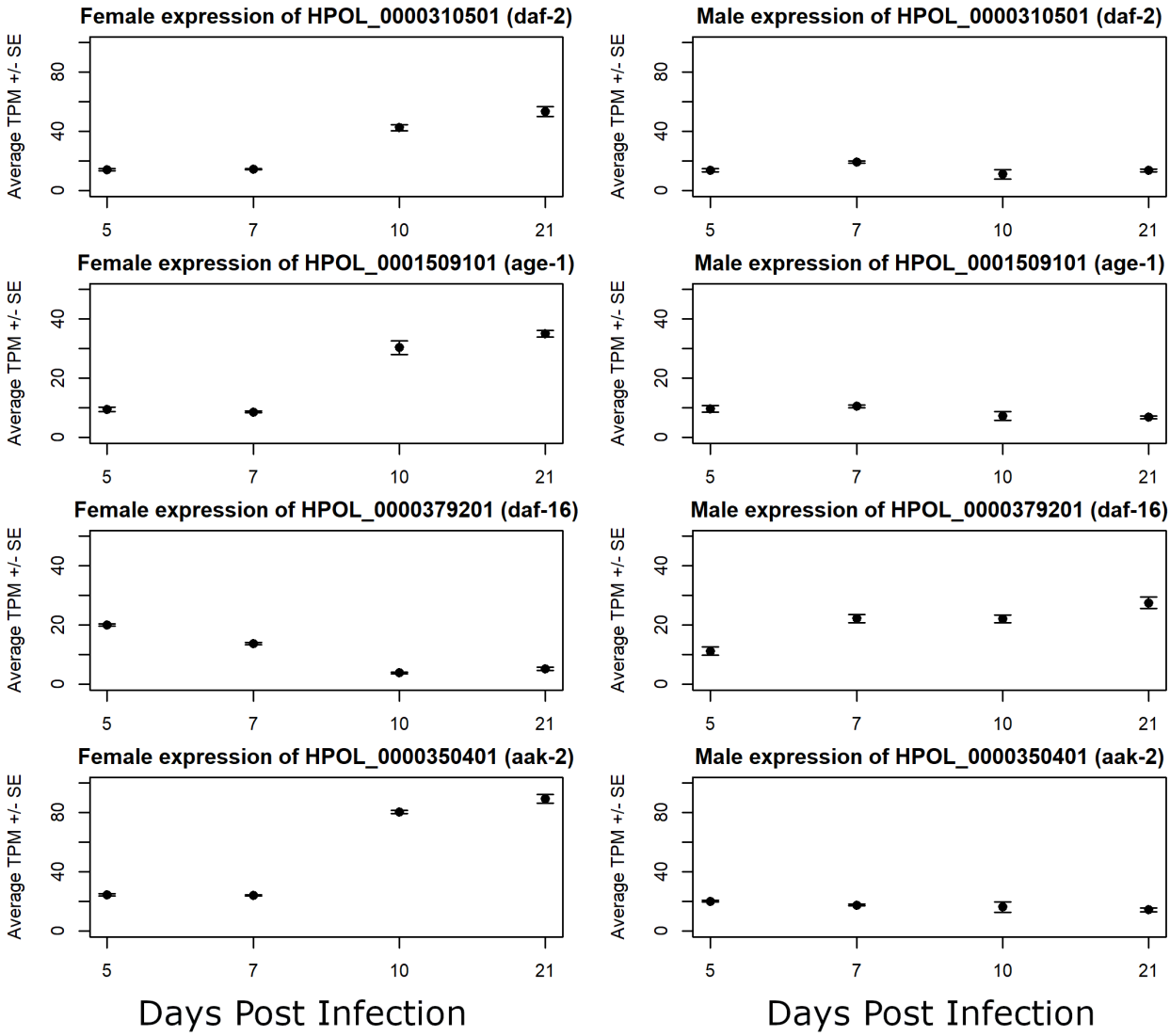
Female expression of HPOL_0000310501 (daf-2)
Male expression of HPOL_0000310501 (daf-2)
Female expression of HPOL_0001509101 (age-1)
Male expression of HPOL_0001509101 (age-1)
Female expression of HPOL_0000379201 (daf-16)
Male expression of HPOL_0000379201 (daf-16)
Female expression of HPOL_0000350401 (aak-2)
Male expression of HPOL_0000350401 (aak-2)
Average TPM +/- SE
0
20
40
80
5
7
10
21
Days Post Infection

Figure 8

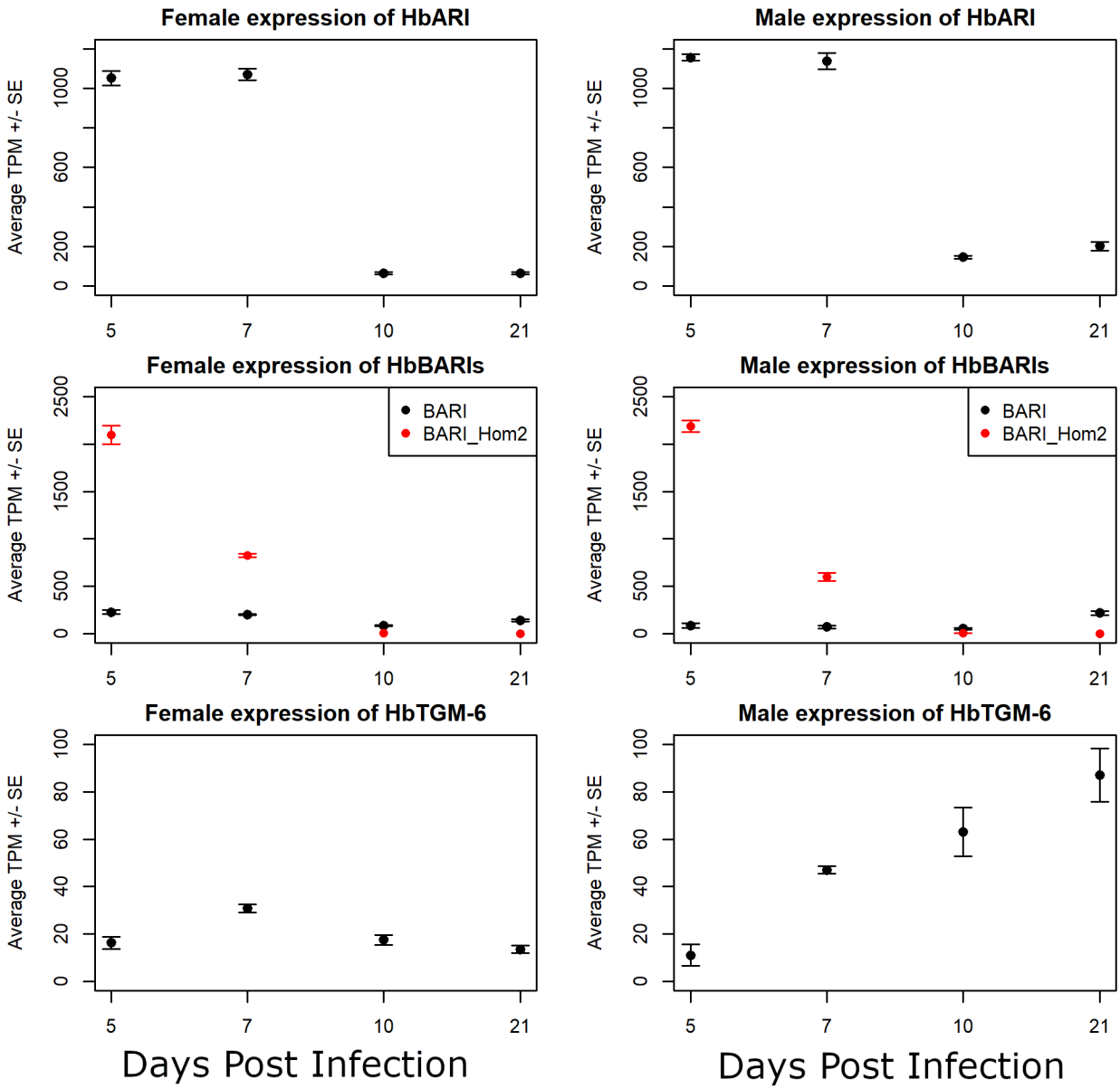
Female expression of HbARI
Male expression of HbARI
Female expression of HbBARIs
Male expression of HbBARIs
Female expression of HbTGM-6
Male expression of HbTGM-6
Average TPM +/- SE
BARI
BARI_Hom2
Days Post Infection

Figure 9

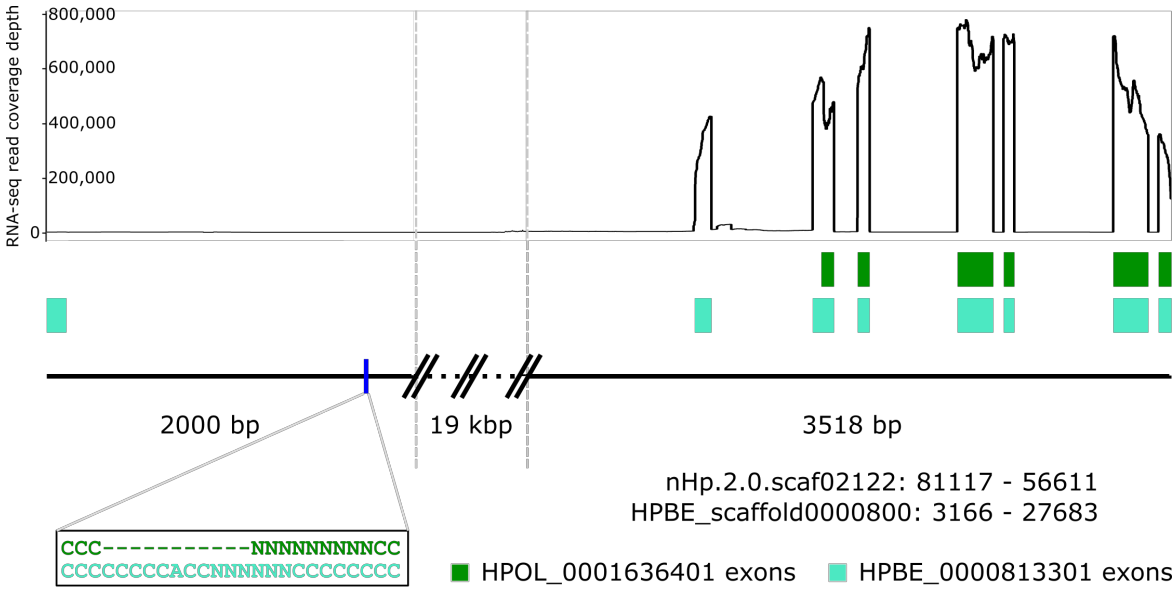
RNA-seq read coverage depth
800,000
600,000
400,000
200,000
0
2000 bp
19 kbp
3518 bp
nHp.2.0.scaf02122: 81117 - 56611
HPBE_scaffold0000800: 3166 - 27683
CCC----------NNNNNNNNNCC
CCCCCCCCACCNNNNNNCCCCCCCC
HPOL_0001636401 exons
HPBE_0000813301 exons